Single and Multi Particle Out-of-Equilibrium Quantum Dynamics for Dephased Long-Range Hopping Lattice Systems

A Thesis

submitted to
Indian Institute of Science Education and Research Pune
in partial fulfillment of the requirements for the
BS-MS Dual Degree Programme

by

Lokesh Tater

Indian Institute of Science Education and Research Pune
Dr. Homi Bhabha Road,
Pashan, Pune 411008, INDIA.

March, 2025

Supervisor: Dr. Bijay K Agarwalla
© Lokesh Tater 2025

All rights reserved

Certificate

This is to certify that this dissertation entitled Single and Multi Particle Out-of-Equilibrium Quantum Dynamics for Dephased Long-Range Hopping Lattice Systems towards the partial fulfilment of the BS-MS dual degree programme at the Indian Institute of Science Education and Research, Pune represents study/work carried out by Lokesh Tater at Indian Institute of Science Education and Research under the supervision of Dr. Bijay K Agarwalla, Associate Professor, Department of Physics , during the academic year 2024-2025.

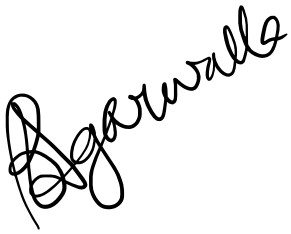

Dr. Bijay K Agarwalla

Committee:

Dr. Bijay K Agarwalla

Dr. M.S. Santhanam

Declaration

I hereby declare that the matter embodied in the report entitled Single and Multi Particle Out-of-Equilibrium Quantum Dynamics for Dephased Long-Range Hopping Lattice Systems are the results of the work carried out by me at the Department of Physics, Indian Institute of Science Education and Research, Pune, under the supervision of Dr. Bijay K Agarwalla and the same has not been submitted elsewhere for any other degree.

Lokesh Tater

Publication

The work entailed in this thesis has resulted in the following publication.

1. L. Tater, S. Sarkar, D.S. Bhakuni and B.K. Agarwalla, "Bipartite particle number fluctuations in dephased long-range lattice systems," *arXiv:2503.20356*, Mar 2025.

Acknowledgments

Foremost, I would like to thank my supervisor, Dr. B.K. Agarwalla, for creating the most conducive research environment and for always encouraging me to explore new ideas and techniques. I would to like to thank my group members, Katha Ganguly, for her incredible patience with my questions and her constant encouragement, and Pitambar Bagui, for engaging discussions. Finally, this project would have not been possible without the constant support of my friends, my sibling and my parents.

Abstract

We theoretically study single and multi particle dynamics on long-range hopping one dimensional fermionic and bosonic lattice systems with hopping decaying as a power-law with exponent μ. The lattice is further subjected to local particle number conserving dephasing at each of its sites. In the limit of strong dephasing, we adiabatically eliminate the coherences and obtain effective dynamical equations for the two-point and four-point correlation functions in the site basis. We devise a novel *bond length* representation for the four-point correlator, which holds for the alternating initial state and allows us to numerically simulate four-point correlator dynamics for significantly large system sizes. For single particle dynamics, we find that even moments of the density profile of a single exciton shows one-parameter scaling behaviour in the form of Family-Viscek (FV) scaling for $\mu \geq 1.5$ with diffusive scaling exponents, whilst for $\mu < 1.5$ the moments fail to show FV scaling. For multi particle dynamics, we find that observables such as particle transport and particle number fluctuations show FV scaling with diffusive scaling exponents for $\mu \geq 1.5$ and super-diffusive scaling exponents for $\mu < 1.5$. We further use the bond length representation to analytically derive the exact FV scaling exponents for particle number fluctuation on fermionic tight-binding ($\mu \to \infty$) lattice.

Contents

Abstract **ix**

1 Introduction **1**

2 Method **5**

2.1 Two-point correlator dynamics 6

2.2 Fermionic four-point correlator dynamics 11

2.3 Bosonic four-point correlator dynamics 22

3 Results **29**

3.1 Single particle dynamics 29

3.2 Fermionic multi particle dynamics 36

3.3 Bosonic multi particle dynamics 46

A Approximate generator for tight-binding fermionic bond length equations **59**

B Particle number fluctuation dynamics in closed long-range hopping lattices **61**

C Initial state dependence of particle number fluctuation dynamics **65**

Chapter 1

Introduction

The Eigenstate Thermalization Hypothesis (ETH) predicts that generic many-body quantum systems, with bulk dephasing, inevitably equilibrate to an infinite temperature thermal state [1, 2]. The non-equilibrium dynamics of such thermalization processes entails rich physics, and can be used to establish universality class of the transport phenomenon of the system. Indeed, the universal properties of non-equilibrium dynamics of local and non-local observables in many-body systems has been a subject of great interest [3–14]. For initial states without large scale density variations, the local observables relax in a system size independent time scales which can predicted via emergence of hydrodynamics in many-body quantum systems [3, 5, 7, 15]. However, the relaxation of non-local observables extends beyond this framework, and typically exhibit much slower and system size dependent time scales [16–22]. Recent theoretical as well as experimental efforts have tried to understand the non-equilibrium dynamics and subsequent equilibration of non-local observables through the frameworks of quantum generalized hydrodynamics [18] and fluctuating hydrodynamics [9, 11]. A key non-local observable to study out-of-equilibrium dynamics is the particle number fluctuation, which quantifies the variance in particle densities in a finite domain of the system [23–29, 29–36]. Many recent works have used particle number fluctuation in contexts such as quantum surface roughening dynamics [37–40], entanglement entropy dynamics [23–25, 29], many-body localization [29–36], characterization of dynamical phase transitions [26–28], among others.

Interaction of quantum systems with the environment leads to dephasing in the form of decoherence, which affects the dynamics of local as well as non-local observables and their corresponding scaling behaviours [41–46]. However, research in this direction has hitherto been limited to short-range hopping systems [11, 37, 38, 47], leaving open questions about dynamics of number fluctuation in long-range hopping systems with power-law hopping and environmental interactions.

Long-range systems exhibit significant qualitative changes in equilibrium phases, ground state properties, and dynamics [48–59] leading to rich and unconventional physics, such as measurement-induced entanglement transitions [60–62] and transitions from normal to anomalous transport in steady-state currents under bulk dephasing [63, 64]. Long-range systems with hopping strength decreasing as a power-law with distance ($\sim 1/r^{\mu}$) are prevalent in natural and artificial light harvesting systems [65–69], and can be engineered in experimental setups [70, 71]. We model such a lattice setup, say with L sites, via the Hamiltonian [58, 63, 64, 72],

$$\hat{H} = J \sum_{i=1}^{L} \sum_{j>i}^{L} \frac{1}{d(i,j)^{\mu}} \Big[\hat{c}_i \hat{c}_j^{\dagger} + \hat{c}_i^{\dagger} \hat{c}_j \Big]. \tag{1.1}$$

Where, $\hat{c}_i(\hat{c}_i^{\dagger})$ denotes the fermionic or bosonic annihilation(creation) operator at lattice site i. J is the hopping strength and μ is the power-law hopping exponent. $d(i,j)$ denotes the distance between lattice sites i and j, and for periodic boundary conditions, is given as $d(m,n) = \min(|i,j|, L - |i-j|)$. Throughout this thesis, we adopt the natural units, $\hbar = c = 1$. We further consider a particle number conserving dephasing probe at each site of the lattice [47, 58, 63, 64, 73–81]. Such a local dephasing can arise from thermal noise or local coupling to the vibrational degrees of freedom [82]. We model the dynamics of the open lattice system setup by the Lindblad quantum master equation (LQME) [83],

$$\frac{d}{dt}\hat{\rho}(t) = \mathcal{L}[\hat{\rho}] = -i\Big[\hat{H}, \hat{\rho}(t)\Big] + \gamma \sum_{j=1}^{L} \Big(\hat{n}_j \, \hat{\rho}(t) \, \hat{n}_j - \frac{1}{2}\{\hat{n}_j^2, \hat{\rho}(t)\} \Big). \tag{1.2}$$

Where, $\rho(t)$ denotes the system density matrix and the jump operator $\hat{n}_i = \hat{c}_i^{\dagger}\hat{c}_i$ is the particle number operator at lattice site i. The first term in Eq. (1.2) represents the unitary (coherence) evolution, whilst the second term represents the Lindbladian dissipation, in the form of on-site (local) dephasing.

Previous studies on such systems have established the existence of a critical value of the

hopping exponent, $\mu_{\rm cr} = d/2 + 1$ (where d is the spacial dimension) below which the system exhibits a distinct phase [58, 62–64]. Such studies have either been in the single exciton limit [58, 64] or have been in the context of steady states of the system [62, 63]. However, the criticality of the hopping exponent μ in the context of multi-particle dynamics remains to be elucidated.

Bipartite particle number fluctuation $w(L,t)$ is defined on a one-dimensional (bosonic or fermionic) lattice with L sites as $w(L,t) = \left\langle \hat{h}^2 \right\rangle - \left\langle \hat{h} \right\rangle^2$, where the operator $\hat{h} = \sum_{i=1}^{L/2} \hat{n}_i$ counts the number of particles in one-half the lattice system. Fujimoto et.al. [11, 37, 38, 47] have established number fluctuation as an excellent candidate to study multi particle dynamics on one-dimensional lattices with conserved total particle number, and have found that in tight-binding ($\mu \to \infty$) lattice systems, bipartite particle number fluctuation dynamics show one-parameter scaling in the form Family-Vicsek (FV) scaling [84–86]:

$$w(L,t) = L^{\alpha} f\left(\frac{t}{L^z}\right), \tag{1.3}$$

where, the scaling function $f(y)$ satisfies the limiting behaviour

$$f(y) \sim \begin{cases} y^{\beta} & \text{for} \quad y \ll 1 \\ 1 & \text{for} \quad y \gg 1 \end{cases}$$

with $\beta = \alpha/z$. This implies the scaling $w(L,t) \sim t^{\beta}$ in the limit $t \ll t^* \sim L^z$. In the absence of dephasing, the scaling exponents fall in the ballistic class ($\alpha = z = 1$) [11, 38], whilst in the presence of dephasing the transport is diffusive and the scaling exponents fall in the so-called Edwards-Wilkinson (EW) class ($\alpha = z/2 = 1$) [47]. FV scaling of bipartite particle number fluctuation in long-range lattices and the impact of long-range hopping on the scaling exponents remains to be shown and forms one of the main questions of this project.

In this project, we study single and multi particle out-of-equilibrium dynamics on one-dimensional long-range fermionic and bosonic lattices, via establishing spatio-temporal scaling of relevant observables. To study single particle dynamics, we consider the moments of the density profile of a single exciton, whilst multi-particle dynamics is studied via observables such as particle transport (comprising of local correlators) and bipartite particle number fluctuation (comprising of non-local correlators).

All observables of our interest can be written in terms of two-point and/or four-point correlators in the site basis. In chapter 2, considering strong dephasing ($\gamma \gg J$), we obtain effective equations of the correlators and develop the *bond length* representation for the effective equations of the four-point correlators. This representation allows us to simulate four-point correlator dynamics for significantly large system sizes ($\approx 10^4$ sites), which has hitherto been a computational challenge. We present our results for fermionic and bosonic single particle dynamics in section 3.1 and find that even-moments of the density profile show FV scaling with diffusive scaling exponents for $\mu \geq 1.5$, whilst for $\mu < 1.5$ the moments fail to show FV scaling. The results for fermionic and bosonic multi particle dynamics is presented in sections 3.2 and 3.3, respectively. We report that particle transport and number fluctuations show universal behaviour in the form of FV scaling for all values of hopping exponent μ, whilst the criticality of μ appears in the values of the scaling exponents α, β and z. We find a crossover from super-diffusive $(\alpha, \beta, z = 1, 1/(2\mu - 1), 2\mu - 1)$ dynamics to diffusive dynamics $(\alpha, \beta, z = 1, 0.5, 2)$ at the critical value of the hopping exponent $\mu_{\text{cr}} \sim 1.5$. We further used the bond length representation to analytically derive the exact FV scaling exponents for dephased fermionic lattices in the short range ($\mu \to \infty$) limit. Our results thus illustrate the Family-Viscek universality of non-equilibrium phenomenon for dephased long-range lattice systems, where the value of the scaling exponents entail information of the universality class. Notably, all observables of our interest are experimentally accessible through quantum simulators [8, 9, 70, 71, 87–95].

Chapter 2

Method

The long-range hopping one-dimensional lattice system, consisting of L sites, with hopping strength decreasing as a power-law, can be modelled by the Hamiltonian,

$$\hat{H} = J \sum_{i=1}^{L} \sum_{j>i}^{L} \frac{1}{d(i,j)^{\mu}} \Big[\hat{c}_i \hat{c}_j^{\dagger} + \hat{c}_i^{\dagger} \hat{c}_j \Big], \tag{2.1}$$

where, $d(i,j)$ denotes the distance between lattice sites indexed by i and j, J is the hopping strength and μ is the power-law hopping exponent. Each lattice site is further subject to local particle number conserving dephasing. Given that the mixed state of the system is described the the density matrix $\hat{\rho}(t)$, the system dynamics can be represented by the Lindblad Quantum Master Equation(LQME), $d\hat{\rho}/dt = \mathcal{L}[\hat{\rho}]$, where $\mathcal{L}[*]$ is the Lindblad super-operator, given by:

$$\mathcal{L}[\hat{\rho}(t)] = -i \Big[\hat{H}, \hat{\rho}(t) \Big] + \gamma \sum_{j=1}^{L} \Big(\hat{n}_j \, \hat{\rho}(t) \, \hat{n}_j - \frac{1}{2} \{ \hat{n}_j^2, \hat{\rho}(t) \} \Big). \tag{2.2}$$

Here, the jump operators $\hat{n}_i = \hat{c}_i^{\dagger} \hat{c}_i$ is the particle number operator at lattice site i, with $\hat{c}_i(\hat{c}_i^{\dagger})$ being the fermionic or bosonic annihilation(creation) operator. Each lattice site is, thus, subject to local particle number conserving dephasing of homogeneous strength γ. The equation of motion of expectation value of an observable $\langle \hat{A} \rangle(t) = \mathrm{Tr} \Big[\hat{\rho}(t) \hat{A} \Big]$ may be

obtained as,

$$\frac{d}{dt}\langle\hat{A}\rangle = \mathrm{Tr}\left[\hat{A}\cdot\frac{d\hat{\rho}}{dt}\right] = -i\left\langle[\hat{A},\hat{H}]\right\rangle + \sum_{i=1}^{L}\gamma\left(\left\langle\hat{n}_i\hat{A}\hat{n}_i\right\rangle - \frac{1}{2}\left\langle\left\{\hat{n}_i^2,\hat{A}\right\}\right\rangle\right), \tag{2.3}$$

Dynamics of thermalization

The LQME Eq. (2.2) conserves the total particle number in the system, i.e, $\sum_{i=1}^{L}\mathrm{Tr}[\hat{n}_i\hat{\rho}(t)] = N$ is a constant of motion. Since the system dynamics remains confined to a fixed particle number Hilbert space $\mathcal{H}_N$, which is dictated by the initial condition $\hat{\rho}(t=0)$. Note that, $\dim\mathcal{H}_N = \binom{L}{N}$.

Further, due to the local particle number dephasing, the system undergoes decoherence in the site basis in time scale $1/\gamma$, controlled by the strength of dephasing. That is, the off-diagonals of the density matrix $\hat{\rho}$ written in the site basis vanish in time scale $1/\gamma$. The steady state of Eq. (2.2) is the maximally mixed state, i.e., $d\hat{\rho}/dt = 0$ for $\hat{\rho}\propto\mathbb{I}$, where $\mathbb{I}$ denotes the identity matrix in the Hilbert space $\mathcal{H}$. Under the conditions of strong dephasing ($\gamma\gg J$), the coherences(off-diagonals) of the density matrix die out much before the system relaxes to the maximally mixed state.

2.1 Two-point correlator dynamics

The two point correlator $D_{mn}(t)$ is defined as, $D_{mn}(t) = \mathrm{Tr}\left[\hat{\rho}(t)\hat{c}_m^\dagger\hat{c}_n\right]$. Here, $\hat{c}_m$ denotes the bosonic or fermionic annihilation operator at site m. The equations of motion of $D_{mn}(t)$ may be obtained using Eq. (2.3). It is important to note that given the quadratic nature of the Hamiltonian and the Lindblad jump operators, the fermionic and bosonic equations of motion of $D_{mn}(t)$ are identical. Hence the analysis that follows in this section holds for fermions as well as bosons. The equation of motion of $D_{mn}(t)$ is given as,

$$\begin{aligned}\frac{d}{dt}D_{mn} &= -i\langle\left[\hat{c}_m^\dagger\hat{c}_n,\hat{H}\right]\rangle + \sum_{i=1}^{L}\gamma\left(\langle\hat{n}_i\hat{c}_m^\dagger\hat{c}_n\hat{n}_i\rangle_t - \frac{1}{2}\langle\{\hat{n}_i^2,\hat{c}_m^\dagger\hat{c}_n\}\rangle\right)\\ &= iJ\sum_{j=\pm1}^{\pm(L/2-1),L/2}\frac{D_{m(n+j)} - D_{(m+j)n}}{|j|^\mu} + \gamma\,(\delta_n^m - 1)D_{mn}.\end{aligned} \tag{2.4}$$

Here we have assumed periodic boundary conditions on the lattice and the site indices are understood to be in mod L arithmetic. The number of independent variables in the above set of equations is L^2. To understand the effect of dephasing, it is worth transforming these equation to the momentum basis defined by the Fourier transform,

$$\tilde{D}_{k_1k_2} = \mathcal{F}[D_{mn}] = \frac{1}{L}\sum_{m,n=0}^{L-1} e^{-\frac{2\pi i}{L}(k_1m+k_2n)} D_{mn}. \tag{2.5}$$

The equation of motion in the momentum basis can be obtained as follows,

$$\begin{aligned}\frac{d}{dt}\tilde{D}_{k_1k_2} &= \frac{1}{L}\sum_{m,n=0}^{L-1} e^{-\frac{2\pi i}{L}(k_1m+k_2n)} \frac{d}{dt}D_{mn} \\ &= i(E(k_1)-E(k_2))\tilde{D}_{k_1k_2} + \frac{1}{L}\sum_{m,n=0}^{L-1} e^{-\frac{2\pi i}{L}(k_1m+k_2n)}\gamma(\delta^n_m - 1)D_{mn}.\end{aligned} \tag{2.6}$$

The first term in the above equation represents the unitary(coherence) evolution, whilst the second term represents the Lindbladian dissipation. $E(k)$ is the spectrum of the long-range hopping Hamiltonian $\hat{H}$ (Eq. (2.1)), given as,

$$E(k) = 2\sum_{j=1}^{L/2-1} \frac{\cos(2\pi kj/L)}{j^\mu} + \frac{e^{i\pi k}}{(L/2)^\mu} \tag{2.7}$$

The second term in Eq. (2.6) can be solved as,

$$\begin{aligned}\frac{d}{dt}\tilde{D}_{k_1k_2} &= i(E(k_1)-E(k_2))\tilde{D}_{k_1k_2} - \frac{\gamma}{L}\sum_{m,n=0}^{L-1} e^{-\frac{2\pi i}{L}(k_1m+k_2n)} D_{mn} + \frac{\gamma}{L}\sum_{m=0}^{L-1} e^{-\frac{2\pi i}{L}m(k_1+k_2)} D_{mm} \\ &= i(E(k_1)-E(k_2))\tilde{D}_{k_1k_2} - \gamma\tilde{D}_{k_1k_2} + \frac{\gamma}{L^2}\sum_{k_1'k_2'}\sum_{m=0}^{L-1} e^{\frac{2\pi i}{L}m\left[(k_1'+k_2')-(k_1+k_2)\right]}\tilde{D}_{k_1'k_2'}\end{aligned} \tag{2.8}$$

Now, in order to evaluate the summation over m in the above equation, note the following:

$$\frac{1}{L}\sum_{m=0}^{L-1} e^{\frac{2\pi i}{L}m\left[(k_1'+k_2')-(k_1+k_2)\right]} = \begin{cases} 1 & \text{for } (k_1'+k_2')-(k_1+k_2) = 0, L, 2L, \cdots \\ 0 & \text{otherwise}\end{cases} \tag{2.9}$$

Hence the equation of motion of two-point correlators in the momentum basis reads as,

$$\frac{d}{dt}\tilde{D}_{k_1k_2} = i(E(k_1) - E(k_2))\tilde{D}_{k_1k_2} - \gamma\tilde{D}_{k_1k_2} + \frac{\gamma}{L}\sum_{(k_1'+k_2')=(k_1+k_2),(k_1+k_2)\pm L}\tilde{D}_{k_1'k_2'} \tag{2.10}$$

Thus we see that the local particle number dephasing induces scattering such that the mode (k_1', k_2') couples to the mode (k_1, k_2) with the following selection rule:

$$(k_1' + k_2') = (k_1 + k_2) \text{ or } (k_1 + k_2) + L \text{ or } (k_1 + k_2) - L \tag{2.11}$$

2.1.1 Effective equations for two-point correlator dynamics

As noted before, the density matrix $\hat{\rho}(t)$, under the LQME Eq. (2.2) remains confined to a fixed particle number Hilbert space $\mathcal{H}_N$. The density matrix confined to the one-particle Hilbert space $\mathcal{H}_1$, written in the site basis is the transpose of the two point correlation matrix. That is,

$$\langle n|\hat{\rho}|m\rangle = D_{mn}, \tag{2.12}$$

where, $|i\rangle = \hat{c}_i^\dagger|0\rangle$ represents the single particle pure state, with a particle localized at site i.

Thus, under the conditions of strong dephasing $\gamma \gg J$, the off diagonals of the two-point correlator matrix $D_{mn}(m \neq n)$ decay to zero in time scale $1/\gamma$, much before the system achieves equilibrium, and at late times $(t \gg 1/\gamma)$ the dynamics can be effectively described as a classical Markov process involving only the diagonals D_{mm}. Such effective equations can be obtained via adiabatic elimination of the off-diagonals in the slower time scale $\tilde{t} = Jt$. In this time scale, note that for the off-diagonals, $\frac{dD_{mn}}{d\tilde{t}} \ll \frac{\gamma}{J}D_{mn}$. Hence, the strong dephasing assumptions are:

1. $D_{mn} \ll D_{mm} \;\; \forall\, m \neq n$
2. $\frac{dD_{mn}}{d\tilde{t}} \ll \frac{\gamma}{J}D_{mn} \;\; \forall\, m \neq n$

The equation of motion of the two-point correlator off-diagonal D_{mn} is

$$\frac{d}{dt}D_{mn} = iJ\sum_{j=\pm1}^{\pm(L/2-1),L/2}\frac{D_{m(n+j)} - D_{(m+j)n}}{|j|^\mu} - \gamma\, D_{mn} \tag{2.13}$$

Applying the second strong dephasing assumption, the derivative on the LHS may be neglected with respect to the dissipative term on the RHS. Which gives,

$$D_{mn} = \frac{iJ}{\gamma} \sum_{j=\pm 1}^{\pm(L/2-1),L/2} \frac{D_{m(n+j)} - D_{(m+j)n}}{|j|^{\mu}} \tag{2.14}$$

Now, on the RHS, noting the first assumption, the off-diagonals may be neglected with respect to the diagonals. This gives the off-diagonal correlator element D_{mn} in terms of the diagonals D_{mm} and D_{nn},

$$D_{mn} = i\,\frac{J}{\gamma}\left(\frac{D_{mm} - D_{nn}}{|m-n|^{\mu}}\right). \tag{2.15}$$

Now, the microscopic equation of motion of the diagonal D_{mm} reads

$$\frac{d}{dt}D_{mm} = iJ \sum_{j=\pm 1}^{\pm(L/2-1),L/2} \frac{D_{m(m+j)} - D_{(m+j)m}}{|j|^{\mu}} \tag{2.16}$$

Note that on the RHS, only the off-diagonal terms appear. Substituting these with diagonals using Eq. (2.13) gives,

$$\boxed{\frac{d}{dt}D_{mm} = \Lambda \sum_{j=\pm 1}^{\pm(L/2-1),L/2} \frac{D_{(m+j)(m+j)} - D_{mm}}{|j|^{2\mu}}.} \tag{2.17}$$

Here, $\Lambda = 2J^2/\gamma$ may be identified as the effective diffusion constant. Equation (2.17) is a discrete one-dimensional fractional diffusion equation, which effectively describes the dynamics of the two-point correlator diagonals, in time scale $t \gg 1/\gamma$. Fig. 2.1, compares the dynamics of a two-point correlator diagonal obtained via numerical integration of the microscopic equations, Eq. (2.4), and effective equations, Eq. (2.17), of the two-point correlator, under the strong dephasing condition ($\gamma/J = 100$). The dynamics show a perfect collapse at times $\gamma t \gg 1$.

The effective equations Eq. (2.17) are translationally invariant, and hence decouple in the Fourier space. Defining the discrete Fourier transform as,

$$\tilde{D}_k = \frac{1}{\sqrt{L}} \sum_{m=1}^{L} e^{-\frac{2\pi i}{L}mk}\, D_{mm}, \tag{2.18}$$

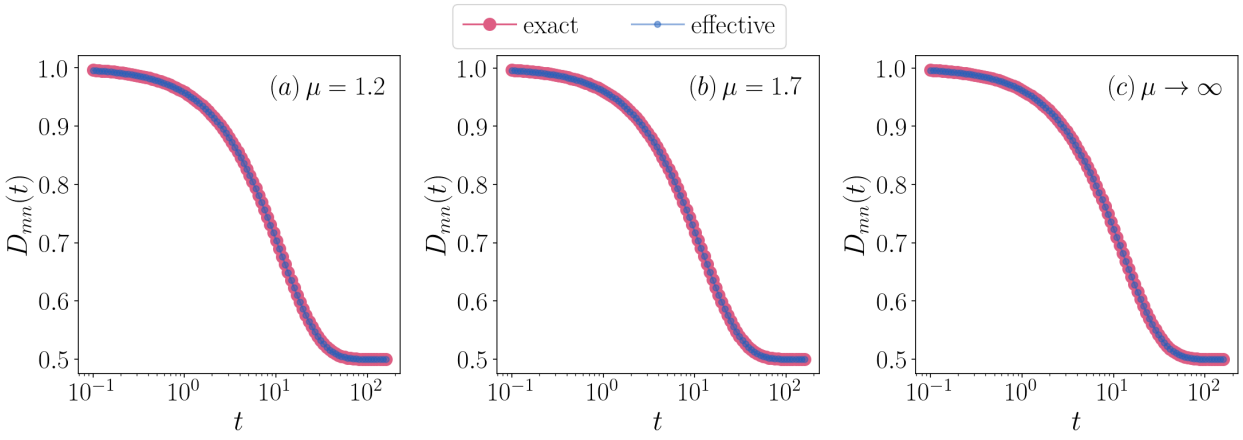

Figure 2.1: Plot for dynamics of a two-point correlator diagonal $D_{mm}(t) = \langle \hat{c}_m^\dagger \hat{c}_m \rangle$ $(m = 0)$, obtained via numerical integration of the microscopic equations (Eq. (2.4)) and effective equations (Eq. (2.17)) of the two-point correlator, for three different values of hopping exponent μ (a)$\mu = 1.2$, (b)$\mu = 1.7$ and (c)$\mu \to \infty$. Lattice size $L = 32$ and dephasing strength $\gamma = 100 * J$. Dynamics start from the alternating initial state $|\psi_{\text{alt}}\rangle = \prod_{m=1}^{L/2} \hat{c}_{2m}^\dagger |0\rangle$

where, $k \in \{0, 1, \cdots, L-1\}$. The equation of motion of the Fourier modes $\tilde{D}_k$ can be obtained as,

$$\begin{aligned}
\frac{d}{dt}\tilde{D}_k &= \frac{1}{\sqrt{L}} \sum_{m=1}^{L} e^{-\frac{2\pi i}{L} mk} \frac{d}{dt} D_{mm} \\
&= \Lambda \sum_{j=\pm 1}^{\pm(L/2-1), L/2} \frac{1}{|j|^{2\mu}} \frac{1}{\sqrt{L}} \sum_{m=1}^{L} e^{-\frac{2\pi i}{L} mk} \left(D_{(m+j)(m+j)} - D_{mm} \right) \\
&= \Lambda \sum_{j=\pm 1}^{\pm(L/2-1), L/2} \frac{1}{|j|^{2\mu}} \left(e^{\frac{2\pi i}{L} jk} - 1 \right) \tilde{D}_k.
\end{aligned} \tag{2.19}$$

As expected, the effective equations decouple in the Fourier basis, and the Fourier modes decay as,

$$\boxed{\tilde{D}_k(t) = e^{-E(k)t} \tilde{D}_k(0),} \tag{2.20}$$

where, the spectrum of the effective equation, Eq. (2.17), $E(k)$ is given by,

$$E(k) = \Lambda \left(4 \sum_{j=1}^{\frac{L}{2}-1} \frac{\sin^2(\pi jk/L)}{j^{2\mu}} + \frac{1 - e^{i\pi k}}{(L/2)^{2\mu}} \right). \tag{2.21}$$

The only non-decaying mode of this spectrum is the lowest lying $k = 0$ mode, since, $E(k = 0) = 0$ and $E(k) > 0$ for $k > 0$. Hence, the two-point correlator matrix equilibrates to:

$$\begin{aligned} D_{mm}(t \to \infty) &= \frac{1}{\sqrt{L}} \sum_{k=0}^{L-1} e^{-\frac{2\pi i}{L} mk} \delta_k^0 \tilde{D}_{k=0}(t=0) \\ &= \frac{1}{\sqrt{L}} \tilde{D}_{k=0}(t=0) \end{aligned} \tag{2.22}$$

2.2 Fermionic four-point correlator dynamics

The four point correlator on a fermionic lattice in the site basis is defined as:

$$F_{mnpq}(t) = \mathrm{Tr}\big[\rho(t)\hat{c}_m^\dagger \hat{c}_n^\dagger \hat{c}_p \hat{c}_q\big] \tag{2.23}$$

where $\hat{c}_m(\hat{c}_m^\dagger)$ is the fermionic annihilation(creation) operator at site m. Fermionic anti-commutation sets correlators of the form F_{mmpq} and F_{mnpp} to zero at all times. For the four-point correlator F_{mnpq}, with $(m \neq n)$ and $(p \neq q)$, the dynamical equation can be obtained via Eq. (2.3), as follows:

$$\begin{aligned} \frac{d}{dt} F_{mnpq} &= -i\langle \Big[\hat{c}_m^\dagger \hat{c}_n^\dagger \hat{c}_p \hat{c}_q, \hat{H}\Big]\rangle + \sum_{i=1}^{L} \gamma \left(\langle \hat{n}_i \hat{c}_m^\dagger \hat{c}_n^\dagger \hat{c}_p \hat{c}_q \hat{n}_i \rangle_t - \frac{1}{2} \langle \big\{ \hat{n}_i^2, \hat{c}_m^\dagger \hat{c}_n^\dagger \hat{c}_p \hat{c}_q \big\} \rangle \right) \\ &= i\, J \sum_{j=\pm 1}^{\pm(L/2-1), L/2} \frac{(1-\delta_q^{p+j}) F_{mn(p+j)q} + (1-\delta_{q+j}^{p}) F_{mnp(q+j)}}{|j|^\mu} \\ &\quad - iJ \sum_{j=\pm 1}^{\pm(L/2-1), L/2} \frac{(1-\delta_n^{m+j}) F_{(m+j)npq} + (1-\delta_{n+j}^{m}) F_{m(n+j)pq}}{|j|^\mu} \\ &\quad + \gamma\, (\delta_m^p + \delta_m^q + \delta_n^p + \delta_n^q - 2) F_{mnpq}. \end{aligned} \tag{2.24}$$

The $(1-\delta_n^m)$ factors appear on the RHS of the Eq. (2.24) due to Fermionic anti-commutation relations, which sets the four-point correlators of the form F_{mmpq} and F_{mnpp} to zero. The $(1-\delta_n^m)$ factors prevent such correlators from appearing in Eq. (2.24). The last term on the RHS of Eq. (2.24) represents the dissipation due to the local particle number dephasing on the lattice.

2.2.1 Effective equations for Fermionic four-point correlator dynamics

The four-point correlators are, in fact, elements of the system density matrix $\rho(t)$, confined to the two-particle Hilbert space $\mathcal{H}_2$. In the two-particle site basis $\{|mn\rangle\}$, where $|mn\rangle = \hat{c}_m^\dagger \hat{c}_n^\dagger |0\rangle$ and $(m \neq n)$,

$$\langle mn|\hat{\rho}|pq\rangle = F_{mnpq} \tag{2.25}$$

Fermionic anti-commutation relations confers the following symmetries on the four-point correlator:

$$F_{mnpq} = -F_{nmpq} = -F_{mnqp} = F_{nmqp} \tag{2.26}$$

Hence, there exists $\binom{L}{2}^2$ independent four-point correlators. Of these, $\binom{L}{2}$ are the diagonals of the four-point correlation matrix, identified as the diagonals of the two-particle density matrix in the two-particle site basis, of the form F_{mnmn} or F_{mnnm}, where $m \neq n$. The microscopic equation of motion for these diagonals is given as,

$$\begin{aligned}\frac{d}{dt}F_{mnmn} = i\,J \sum_{j=\pm 1}^{\pm(L/2-1),L/2} \frac{(1-\delta_n^{m+j})F_{mn(m+j)n} + (1-\delta_{n+j}^{m})F_{mnm(n+j)}}{|j|^\mu} \\ - iJ \sum_{j=\pm 1}^{\pm(L/2-1),L/2} \frac{(1-\delta_n^{m+j})F_{(m+j)nmn} + (1-\delta_{n+j}^{m})F_{m(n+j)mn}}{|j|^\mu}\end{aligned} \tag{2.27}$$

The off-diagonals of the four-point correlation matrix F_{mnpq} can be categorized as follows: (i) Only one element of pair (m,n) matches with pair (p,q) i.e., either $m=p$, or $m=q$, or $n=p$, or $n=q$. (ii) No element of pair (m,n) matches with pair (p,q). Note that in the equation for the diagonals F_{mnmn} (Eq. (2.27)), only the off-diagonals of type 1 (i.e., $F_{mnm(n+j)}, F_{mnn(m+j)}, F_{(m+j)nmn}$ or $F_{m(n+j)mn}$, with $j \neq 0$) appear on the RHS. The equation of motion of these off-diagonals is given as follows:

$$\begin{aligned}\frac{d}{dt}F_{mnm(n+j)} = \; & iJ \sum_{j'=\pm 1}^{\pm(L/2-1),L/2} \frac{(1-\delta_{n+j}^{m+j'})F_{mn(m+j')(n+j)} + (1-\delta_{n+j+j'}^{m})F_{mnm(n+j+j')}}{|j'|^\mu} \\ & - iJ \sum_{j'=\pm 1}^{\pm(L/2-1),L/2} \frac{(1-\delta_n^{m+j'})F_{(m+j')nm(n+j)} + (1-\delta_{n+j'}^{m})F_{m(n+j')m(n+j)}}{|j'|^\mu} \\ & - \gamma F_{mnm(n+j)}\end{aligned} \tag{2.28}$$

$$\frac{d}{dt}F_{mn(m+j)n} = iJ\sum_{j'=\pm1}^{\pm(L/2-1),L/2}\frac{(1-\delta_n^{m+j+j'})F_{mn(m+j+j')n}+(1-\delta_{n+j}^{m+j'})F_{mn(m+j')(n+j)}}{|j'|^\mu} - iJ\sum_{j'=\pm1}^{\pm(L/2-1),L/2}\frac{(1-\delta_n^{m+j'})F_{(m+j')n(m+j)n}+(1-\delta_{n+j'}^{m})F_{m(n+j')(m+j)n}}{|j'|^\mu} - \gamma F_{mn(m+j)n} \tag{2.29}$$

$$\frac{d}{dt}F_{(m+j)nmn} = iJ\sum_{j'=\pm1}^{\pm(L/2-1),L/2}\frac{(1-\delta_n^{m+j'})F_{(m+j)n(m+j')n}+(1-\delta_{n+j'}^{m})F_{(m+j)nm(n+j')}}{|j'|^\mu} - iJ\sum_{j'=\pm1}^{\pm(L/2-1),L/2}\frac{(1-\delta_n^{(m+j)+j'})F_{((m+j)+j')nmn}+(1-\delta_{n+j'}^{(m+j)})F_{(m+j)(n+j')mn}}{|j'|^\mu} - \gamma F_{(m+j)nmn} \tag{2.30}$$

$$\frac{d}{dt}F_{m(n+j)mn} = iJ\sum_{j'=\pm1}^{\pm(L/2-1),L/2}\frac{(1-\delta_n^{m+j'})F_{m(n+j)(m+j')n}+(1-\delta_{n+j'}^{m})F_{m(n+j)m(n+j')}}{|j'|^\mu} - iJ\sum_{j'=\pm1}^{\pm(L/2-1),L/2}\frac{(1-\delta_{n+j}^{m+j'})F_{(m+j')(n+j)mn}+(1-\delta_{n+j+j'}^{m})F_{m(n+j+j')mn}}{|j'|^\mu} - \gamma F_{m(n+j)mn} \tag{2.31}$$

Under the conditions of strong dephasing ($\gamma \gg J$), the off-diagonals of the four-point correlator matrix vanish, much before the system equilibrates to the maximally mixed state. Hence, in the slower time scale ($\tilde{t} = Jt$), the dynamics can be mapped to a classical Markov process involving the diagonals F_{mnmn}, via adiabatic elimination of the off-diagonals. Denoting the diagonals as $F_{\rm d}$ and the off-diagonals as $F_{\rm off-d}$, the strong dephasing assumptions, valid in time scale $\tilde{t} = Jt$ are:

1. $F_{\rm off-d} \ll F_{\rm d}$
2. $\partial_{\tilde{t}} F_{\rm off-d} \ll \frac{\gamma}{J} F_{\rm off-d}$

Applying the second assumption to Eqs. (2.28) to (2.31), the derivative on LHS of these equations may be neglected. Further, applying the first assumption, the off-diagonals in the

summations on the RHS of these equations may be neglected. This gives the off-diagonals of type (i) in the terms of the diagonals, as follows,

$$\begin{aligned}
F_{(m+j)nmn} &= \frac{iJ}{\gamma}(1-\delta_n^{m+j})\frac{F_{(m+j)n(m+j)n}-F_{mnmn}}{|j|^{\mu}}.\\
F_{m(n+j)mn} &= \frac{iJ}{\gamma}(1-\delta_{n+j}^{m})\frac{F_{m(n+j)m(n+j)}-F_{mnmn}}{|j|^{\mu}}.\\
F_{mn(m+j)n} &= \frac{iJ}{\gamma}(1-\delta_n^{m+j})\frac{F_{mnmn}-F_{(m+j)n(m+j)n}}{|j|^{\mu}}.\\
F_{mnm(n+j)} &= \frac{iJ}{\gamma}(1-\delta_{n+j}^{m})\frac{F_{mnmn}-F_{m(n+j)m(n+j)}}{|j|^{\mu}}.
\end{aligned} \tag{2.32}$$

Substituting the above in the equation of motion of the diagonal F_{mnmn} (Eq. (2.27)), provides the effective equation for the Fermionic four point correlator:

$$\begin{aligned}
\frac{d}{dt}F_{mnmn} &= \Lambda \sum_{j=\pm 1}^{\pm(L/2-1),L/2}(1-\delta_n^{m+j})\frac{F_{(m+j)n(m+j)n}-F_{mnmn}}{|j|^{2\mu}}\\
&= \Lambda \sum_{j=\pm 1}^{\pm(L/2-1),L/2}(1-\delta_{n+j}^{m})\frac{F_{m(n+j)m(n+j)}-F_{mnmn}}{|j|^{2\mu}},
\end{aligned} \tag{2.33}$$

with the constraint $m \neq n$, and $\Lambda = 2J^2/\gamma$ can be identified as the diffusion constant. Fig. 2.2, compares the dynamics of a four-point correlator diagonal obtained via numerical integration of the microscopic equations, Eq. (2.24), and effective equations, Eq. (2.33), of the four-point correlator, under the strong dephasing condition ($\gamma/J = 100$). The dynamics show a perfect collapse at times $\gamma t \gg 1$.

Although Eq. (2.33) appears to be a two-dimensional discrete diffusion equation, the $(1-\delta_n^m)$ factors, appearing due to Fermionic anti-commutation relations, destroy the translational invariance of the equations. This prevents the decoupling of the equations in the Fourier space. The effective equations for the four-point correlator are essentially a classical Markov process amongst the diagonals of two-particle density matrix. Since, the number of diagonals are $\binom{L}{2}$, the size of the generator of these equations grows as $\sim L^4$. This is a significant computational improvement, compared to the microscopic equations for the four-point correlator, where the number of independent variables are $\binom{L}{2}^2$ and the size of the generator grows as $\sim L^8$.

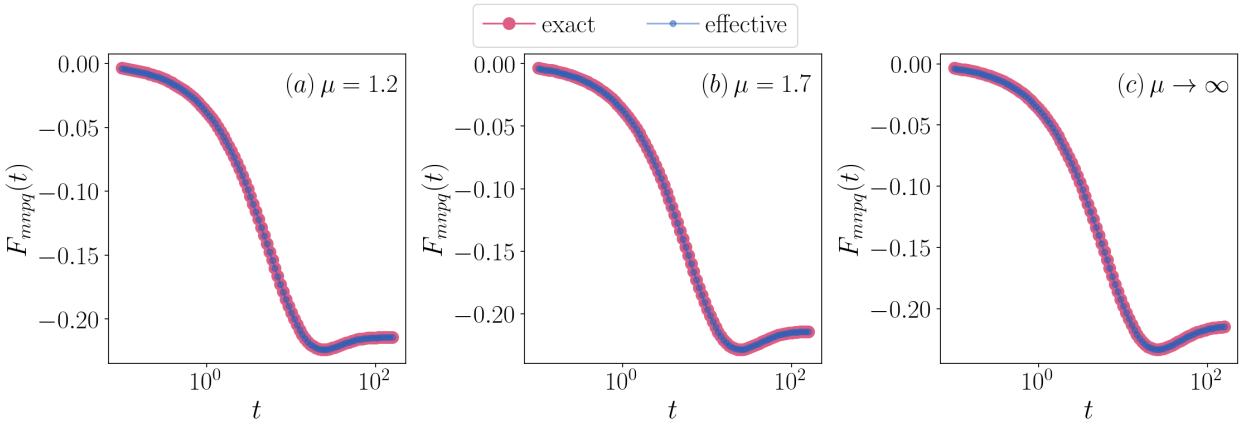

Figure 2.2: Plot for dynamics of a four-point correlator diagonal $F_{mnpq}(t) = \langle \hat{c}_m^\dagger \hat{c}_n^\dagger \hat{c}_p \hat{c}_q \rangle$ with $(m, n, p, q) = (1, L/2, 1, L/2)$, obtained via numerical integration of the microscopic equations (Eq. (2.24)) and effective equations (Eq. (2.33)) of the four-point correlator, for three different values of hopping exponent μ (a)$\mu = 1.2$, (b)$\mu = 1.7$ and (c)$\mu \to \infty$. Lattice size is $L = 8$ and the dephasing strength is $\gamma = 100 * J$. Dynamics start from the alternating initial state $|\psi_{\text{alt}}\rangle = \prod_{m=1}^{L/2} \hat{c}_{2m}^\dagger |0\rangle$

2.2.2 Bond length equations for Fermionic four-point correlators

On a lattice system with L sites, under periodic boundary conditions, the distance $d(m, n)$ between sites m and n is given as, $d(m, n) = \min(|m - n|, L - |m - n|)$. This distance can be defined as the *bond lenght* of the four-point correlator diagonal F_{mnmn}. Note that $d(m, n) \in \{1, 2, \cdots, L/2\}$. For the alternating state $|\psi_{\text{alt}}\rangle = \prod_{m=1}^{L/2} \hat{c}_{2m}^\dagger |0\rangle$, all bonds with $d(m, n)$ being odd have one lattice site occupied and another unoccupied. Whilst for bonds with $d(m, n)$ being even, either both the lattice sites are occupied or both the lattice sites are unoccupied. These points, along with the translational invariance of the effective equations for the four-point correlators (Eq. 2.33) motivate the following claims:

- Given a value $p \in \{1, 3, .., L/2 - 1\}$, the values of all diagonals $F_{mnmn}(t)$ with bond length $d(m, n) = p$ are identical throughout the dynamics, and we label these as $G_p^{(0)}(t)$. That is, $F_{1212} = F_{2323} = \cdots = F_{L1L1} = G_{(1)}^0$, $F_{1414} = F_{2525} = \cdots = F_{(L-3)1(L-3)1} = G_3^{(0)}$ and so on for $p = 5, 7, \cdots, L/2 - 1$

- Given a value $p \in \{2, 4, \cdots, L/2\}$, the values of all diagonals $F_{mnmn}(t)$ with (i) bond length $d(m, n) = p$ and (ii) both sites occupied in the initial state are identical throughout the dynamics, and we label these as $G_p^{(1)}$. That is, $F_{2424} = F_{4646} = \cdots = F_{L2L2} =$

$G_2^{(1)}$, $F_{2626} = F_{4848} = F_{(L-2)2(L-2)2} = G_4^{(1)}$ and so on for $p = 6, 8, \cdots, L/2$.

– Given a value $p \in \{2, 4, \cdots, L/2\}$, the values of all diagonals $F_{mnmn}(t)$ with bond length $d(m, n) = p$ and both sites unoccupied in the initial state are identical throughout the dynamics, and we label these as $G_p^{(2)}$. That is, $F_{1313} = F_{3535} = \cdots = F_{(L-1)1(L-1)1} = G_2^{(2)}$, $F_{1515} = F_{3737} = F_{(L-3)1(L-3)1} = G_4^{(2)}$ and so on for $p = 6, 8, \cdots, L/2$.

The above rules essentially define a bijection between the set of four-point correlator diagonals $\{F_{mnmn}\}$ and the set of bond length variables $\left\{G_p^{(0),(1),(2)}\right\}$. Using this map on Eq. (2.33) and substituting the diagonals F_{mnmn} with the appropriate bond length variables $G_p^{(0),(1),(2)}$ gives,

$$\frac{d}{dt}G_p^{(0)} = 2\,\Lambda \sum_{\substack{p'\to\text{odd}\\ p'\neq p}} U_{pp'}\left(G_{p'}^{(0)} - G_p^{(0)}\right) + 2\,\Lambda \sum_{\substack{p'\to\text{even}\\ p'\neq p}} U_{pp'}\left(\frac{G_{p'}^{(1)} + G_{p'}^{2}}{2} - G_p^{(0)}\right), \tag{2.34}$$

$$\frac{d}{dt}G_p^{(1)} = 2\,\Lambda \sum_{\substack{p'\to\text{odd}\\ p'\neq p}} U_{pp'}\left(G_{p'}^{(0)} - G_p^{(1)}\right) + 2\Lambda \sum_{\substack{p'\to\text{even}\\ p'\neq p}} U_{pp'}\left(G_{p'}^{(1)} - G_p^{(1)}\right), \tag{2.35}$$

$$\frac{d}{dt}G_p^{(2)} = 2\,\Lambda \sum_{\substack{p'\to\text{odd}\\ p'\neq p}} U_{pp'}\left(G_{p'}^{(0)} - G_p^{(2)}\right) + 2\Lambda \sum_{\substack{p'\to\text{even}\\ p'\neq p}} U_{pp'}\left(G_{p'}^{(2)} - G_p^{(2)}\right). \tag{2.36}$$

Here, $\Lambda = 2J^2/\gamma$ is the diffusion constant appearing in Eq. (2.33) and the elements of the coupling matrix $U_{pp'}$ are given as,

$$U_{pp'} = \begin{cases} \frac{1}{|p'-p|^{2\mu}} & \text{if } p' = L/2 \\ \frac{1}{|p'-p|^{2\mu}} + \begin{cases} 1/(p+p')^{2\mu} & \text{if } p+p' \leq L/2 \\ 1/(L-(p+p'))^{2\mu} & \text{if } p+p' > L/2 \end{cases} & \text{if } p' < L/2 \end{cases} \tag{2.37}$$

Now, particle number fluctuations on a domain $\{1, 2, \cdots, M\}$ of the lattice, $w_M(L, t) = \left\langle \hat{h}^2 \right\rangle - \left\langle \hat{h} \right\rangle^2$ where $\hat{h} = \sum_{i=1}^{M} \hat{n}_i$ counts the number of particles in the domain $\{1, 2, \cdots, M\}$,

can be written in terms of the bond length variables as,

$$w_M(L,t) = -\sum_{\substack{p=1\\ p\to\text{odd}}}^{M}(M-p)G_p^{(0)} - \sum_{\substack{p=1\\ p\to\text{even}}}^{M}(M-p)\frac{G_p^{(1)}+G_p^{(2)}}{2} + \sum_{m=1}^{M} D_{mm}\left[1-\sum_{n=1}^{M} D_{nn}\right], \quad (2.38)$$

where $D_{mm} = \left\langle \hat{c}_m^\dagger \hat{c}_m \right\rangle$ are the diagonals of the two-point correlator matrix, as defined in Sec. 2.1. In the above expression of particle number fluctuation, for bonds with even length bond length, the occupied ($G^{(1)}$) and unoccupied ($G^{(2)}$) bonds contribute equally. Hence, for purposes of computing particle number fluctuation, the following representation can be used:

$$G_p = \begin{cases} G_p^{(0)} & \text{for } p \in \text{odd} \\ \frac{G_p^{(1)}+G_p^{(2)}}{2} & \text{for } p \in \text{even} \end{cases} \quad (2.39)$$

The dynamical equations of the bond length variables $\{G_p\}$ can be obtained via averaging Eqs. (2.35) and (2.36), which gives,

$$\boxed{\frac{d}{dt}G_p = 2\,\Lambda \sum_{\substack{p'=1\\ p'\neq p}}^{L/2} U_{pp'}\,(G_{p'} - G_p),} \quad (2.40)$$

where, the coupling matrix $U_{pp'}$ is as defined in Eq. (2.37). Fig. 2.3, compares the dynamics of a four-point correlator diagonal obtained via numerical integration of the microscopic equations (Eq. 2.24) and bond length equations (Eq. 2.40) of the four-point correlator. One observes a perfect collapse between the microscopic and bond length dynamics at all times.

There are $L/2$ independent variables in the above bond length equations, Eq (2.40). As a result, the number of elements in generator of these equations grows as $\sim L^2$. This provides a significant computational advantage in the numerical simulation of number fluctuation dynamics, over the microscopic (Eq. 2.24) and effective equations (Eq. 2.33) of four-point correlator dynamics, where the size of the generator grows as $\sim L^8$ and $\sim L^4$, respectively.

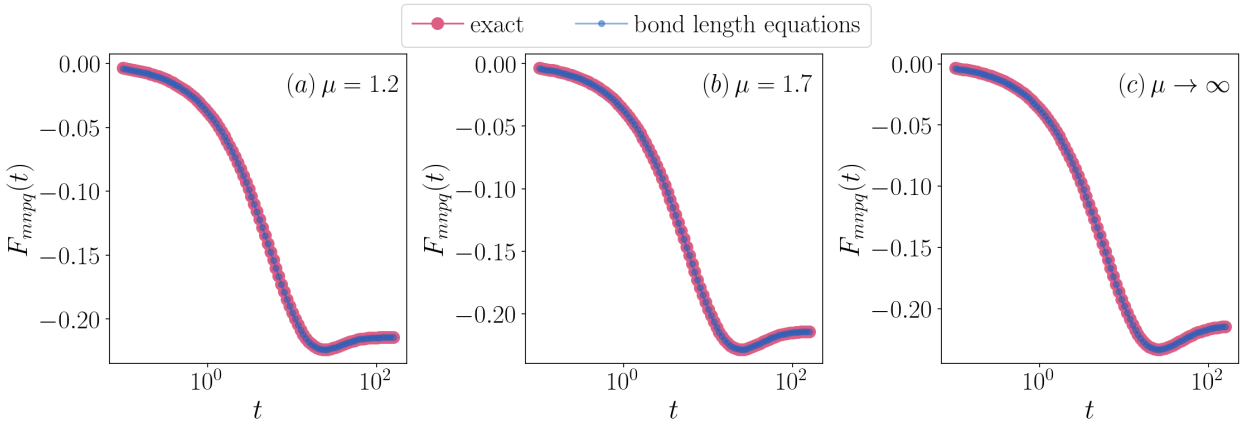

Figure 2.3: Plot for dynamics of a four-point correlator diagonal $F_{mnpq}(t) = \left\langle \hat{c}_m^\dagger \hat{c}_n^\dagger \hat{c}_p \hat{c}_q \right\rangle$ with $(m, n, p, q) = (1, L/2, 1, L/2)$, obtained via numerical integration of the microscopic equations (Eq. (2.24)) and bond length equations (Eq. (2.40)) of the four-point correlator, for three different values of hopping exponent μ (a)$\mu = 1.2$, (b)$\mu = 1.7$ and (c)$\mu \to \infty$. Lattice size $L = 8$ and dephasing strength $\gamma = 100 * J$. Dynamics start from the alternating initial state $|\psi_{\text{alt}}\rangle = \prod_{m=1}^{L/2} \hat{c}_{2m}^\dagger |0\rangle$. One observes a perfect collapse between the dynamics at all times.

Solution for Fermionic bond length equations for tight-binding lattice ($\mu \to \infty$)

The Fermionic bond length equations (Eq. 2.40) can be written as the linear first-order differential equation:

$$\frac{d}{d\tau}|G\rangle = \mathbf{U}_\mu |G\rangle, \tag{2.41}$$

where, $\tau = 2\Lambda t$ and the p-th element of the vector $|G\rangle$ is the bond length variable G_p. For the tight-binding lattice setup (i.e., for hopping exponent $\mu \to \infty$) the generator $\mathbf{U}_{\mu\to\infty}$ is tri-diagonal and is of the form:

$$\mathbf{U}_{\mu\to\infty} = \begin{pmatrix} -1 & 1 & 0 & 0 & \dots & 0 & 0 \\ 1 & -2 & 1 & 0 & \dots & 0 & 0 \\ 0 & 1 & -2 & 1 & \dots & 0 & 0 \\ \dots & \dots & \dots & \dots & \dots & \dots & \dots \\ 0 & 0 & \dots & 1 & -2 & 1 & 0 \\ 0 & 0 & 0 & \dots & 1 & -2 & 1 \\ 0 & 0 & 0 & \dots & 0 & 2 & -2 \end{pmatrix}_{L/2\times L/2} . \tag{2.42}$$

This generator $\mathbf{U}_\mu$ can be symmetrized to $\tilde{\mathbf{U}}_\mu$ by scaling the last row by half, i.e. $\tilde{\mathbf{U}}_\mu = S\mathbf{U}_\mu$, where,

$$S = \begin{pmatrix} 1 & 0 & 0 & \dots & 0 \\ 0 & 1 & 0 & \dots & 0 \\ \dots & \dots & \dots & \dots & \dots \\ 0 & \dots & 0 & 1 & 0 \\ 0 & \dots & 0 & 0 & 0.5 \end{pmatrix}_{L/2\times L/2} \tag{2.43}$$

The symmetrized generator for the tight-binding setup is:

$$\tilde{\mathbf{U}}_{\mu\to\infty} = S\cdot\mathbf{U}_{\mu\to\infty} = \begin{pmatrix} -1 & 1 & 0 & 0 & \dots & 0 & 0 \\ 1 & -2 & 1 & 0 & \dots & 0 & 0 \\ 0 & 1 & -2 & 1 & \dots & 0 & 0 \\ \dots & \dots & \dots & \dots & \dots & \dots & \dots \\ 0 & 0 & \dots & 1 & -2 & 1 & 0 \\ 0 & 0 & 0 & \dots & 1 & -2 & 1 \\ 0 & 0 & 0 & \dots & 0 & 1 & -1 \end{pmatrix}_{L/2\times L/2} . \tag{2.44}$$

It can be shown that the dynamics generated by $\mathbf{U}_{\mu\to\infty}$ and $\tilde{\mathbf{U}}_{\mu\to\infty}$ for a bond length variable G_p, converge in the thermodynamic limit ($L\to\infty$), provided that $p \ll L$ (see appendix A). That is,

$$\lim_{L\to\infty} \langle p|\, e^{\mathbf{U}_{\mu\to\infty}t}\, |G(t=0)\rangle = \lim_{L\to\infty} \langle p|\, e^{\tilde{\mathbf{U}}_{\mu\to\infty}t}\, |G(t=0)\rangle\,, \tag{2.45}$$

where the vector $|p\rangle$, $|p\rangle_j = \delta^j_p$, extracts the p-th element from the dynamics generated by $\mathbf{U}_{\mu\to\infty}$ or $\tilde{\mathbf{U}}_{\mu\to\infty}$. Therefore, the symmetrized generator $\tilde{\mathbf{U}}_{\mu\to\infty}$ can be used to analyse the dynamics of the bond length variables, in the thermodynamic limit.

The symmetrized tight binding generator $\tilde{\mathbf{U}}_{\mu\to\infty}$ can be diagonalized, with eigenvectors $|v^{(k)}\rangle$ and corresponding eigenvalues $\lambda^{(k)}$ [96] given as,

$$\begin{aligned} \lambda^{(k)} &= -2 + 2\cos\left(\frac{2\pi k}{L}\right) = -4\sin^2\left(\frac{\pi k}{L}\right) \\ |v^{(k)}\rangle_j &= \begin{cases} 1/\sqrt{L/2} & \text{for } k = 0 \\ \frac{1}{\sqrt{L/4}}\cos\left(\frac{\pi k(2j-1)}{L}\right) & \text{for } k = 1, 2, \cdots, \frac{L}{2}-1 \end{cases} \end{aligned} \tag{2.46}$$

where, $j = 1, \ldots, L/2$. The bond length vector at time $\tau = 2\Lambda t$, $|G(\tau)\rangle$, is given by:

$$|G(\tau)\rangle = \mathcal{F}^{-1} e^{\mathcal{F}\tilde{U}\mathcal{F}^{-1}\tau} |\tilde{G}(0)\rangle. \tag{2.47}$$

Where $|\tilde{G}(0)\rangle = \mathcal{F}|G(0)\rangle$ is bond length vector in the eigenbasis $\left\{|v^{(k)}\rangle\right\}$, k-th row of $\mathcal{F}$ is the eigenvector $|v^{(k)}\rangle$ and $\mathcal{F}^{-1} = \mathcal{F}^T$. The initial state of the bond length vector can be obtained from the alternating initial condition on the lattice, $|G(0)\rangle_p = 0$ for $p = 1, 3, \cdots, L/2 - 1$ and $|G(0)\rangle_p = -\frac{1}{2}$ for $p = 2, 4, \cdots, L/2$. The initial state in the eigenbasis $\left\{|v^{(k)}\rangle\right\}$ is given as,

$$\begin{aligned}
\tilde{G}_k(\tau = 0) &= |\mathcal{F}|G(0)\rangle\rangle_k = \sum_j |v^{(k)}\rangle_j |G(0)\rangle_j \\
&= \begin{cases} -\frac{L/8}{\sqrt{L/2}} & \text{for } k = 0 \\ -\frac{1}{\sqrt{L}} \cos\left(\frac{\pi k}{L}\right) \sum_{j=1}^{L/4} \cos\left(\frac{\pi k}{(L/4)} j\right) - \frac{1}{\sqrt{L}} \sin\left(\frac{\pi k}{L}\right) \sum_{j=1}^{L/4} \sin\left(\frac{\pi k}{(L/4)} j\right) & \text{for } k \neq 0. \end{cases}
\end{aligned} \tag{2.48}$$

For $k \in \{1, .., L/2 - 1\}$, the summations over cos and sin can be evaluated exactly, to get:

$$\begin{aligned}
\sum_{j=1}^{L/4} \cos\left(\frac{\pi k}{(L/4)} j\right) &= \begin{cases} 0 & \text{if } k \in \text{even} \\ -1 & \text{if } k \in \text{odd} \end{cases} \\
\sum_{j=1}^{L/4} \sin\left(\frac{\pi k}{(L/4)} j\right) &= \begin{cases} 0 & \text{if } k \in \text{even} \\ \cot\left(\frac{2\pi k}{L}\right) & \text{if } k \in \text{odd}. \end{cases}
\end{aligned} \tag{2.49}$$

Therefore at $t = 0$, and for $k \in$ odd, the mode occupancy is:

$$\begin{aligned}
\tilde{G}_k(\tau = 0) &= \frac{1}{\sqrt{L}} \cos\left(\frac{\pi k}{L}\right) - \frac{1}{\sqrt{L}} \sin\left(\frac{\pi k}{L}\right) \frac{\cos(2\pi k/L)}{\sin(2\pi k/L)} \\
&= \frac{1}{\sqrt{L}} \cos\left(\frac{\pi k}{L}\right) - \frac{1}{\sqrt{L}} \sin\left(\frac{\pi k}{L}\right) \frac{\cos(2\pi k/L)}{2\sin(\pi k/L)\cos(\pi k/L)} \\
&= \frac{1}{\sqrt{L}} \left(\frac{2\cos^2(\pi k/L) - \cos(2\pi k/L)}{2\cos(\pi k/L)}\right) \\
&= \frac{1}{\sqrt{L}} \left(\frac{2\cos^2(\pi k/L) - 2\cos^2(\pi k/L) + 1}{2\cos(\pi k/L)}\right) = \frac{1}{2\sqrt{L}} \frac{1}{\cos(\pi k/L)}.
\end{aligned} \tag{2.50}$$

Therefore, to summarize, the initial state of the bond length vector in the eigenbasis $\left\{|v^{(k)}\rangle\right\}$

is,

$$\tilde{G}_k(\tau=0) = \begin{cases} -\sqrt{2L}/8 & \text{for } k=0 \\ \begin{cases} 0 & \text{if } k \in \text{even} \\ \frac{\sec(\pi k/L)}{2\sqrt{L}} & \text{if } k \in \text{odd} \end{cases} & \text{for } k \neq 0. \end{cases} \tag{2.51}$$

Using this result, the bond length variables at time $\tau = 2\Lambda t$ can be obtained as

$$\begin{aligned} G_p(\tau) &= \sum_{k=0}^{L/2-1} \mathcal{F}_{pk}^{-1} e^{\lambda^{(k)}\tau} \tilde{G}_k(\tau=0) \\ &= -\frac{1}{4} + \frac{1}{\sqrt{L/4}} \sum_{k=1}^{L/2-1} \cos\left(\frac{\pi k(2p-1)}{L}\right) e^{\lambda^{(k)}\tau} \tilde{G}_k(\tau=0) \\ &= -\frac{1}{4} + \frac{1}{L} \sum_{k\in\text{odd}} \cos\left(\frac{\pi k(2p-1)}{L}\right) e^{\lambda^{(k)}\tau} \sec\left(\frac{\pi k}{L}\right) \\ &= -\frac{1}{4} + \frac{1}{L} \sum_{k\in\text{odd}} \left(\cos\left(\frac{2\pi pk}{L}\right) + \tan\left(\frac{\pi k}{L}\right)\sin\left(\frac{2\pi pk}{L}\right)\right) e^{\lambda^{(k)}\tau}. \end{aligned} \tag{2.52}$$

At sufficiently late times, low-lying modes ($k \ll L$) dominate the dynamics and higher modes $k \sim \mathcal{O}(L)$ decay to zero. Hence, small angle approximation holds for $\pi k/L$, i.e., the approximations (i) $\lambda^{(k)} \approx -4\pi^2 k^2/L^2$, (ii) $\tan(\pi k/L) \approx \pi k/L$ hold, and one obtains,

$$\begin{aligned} G_p(t) &\approx -\frac{1}{4} + \frac{1}{L} \sum_{k\in\text{odd}} \left(\cos\left(\frac{2\pi pk}{L}\right) + \frac{\pi k}{L}\sin\left(\frac{2\pi pk}{L}\right)\right) e^{-\frac{4\pi^2k^2}{L^2}\tau} \\ &\approx -\frac{1}{4} + \frac{1}{L} \sum_{k\in\text{odd}} \cos\left(\frac{2\pi pk}{L}\right) e^{-\frac{4\pi^2k^2}{L^2}\tau} \end{aligned}. \tag{2.53}$$

The second term on the RHS is denoted as $H_p(\tau)$, and is solved as follows,

$$\begin{aligned} H_p(\tau) &= \frac{1}{L} \sum_{k\in\text{odd}} \cos\left(\frac{2\pi pk}{L}\right) e^{-\frac{4\pi^2k^2}{L^2}\tau} \\ &= \frac{1}{L} \sum_{k=0}^{L/2-1} \cos\left(\frac{2\pi pk}{L}\right) e^{-\frac{4\pi^2k^2}{L^2}\tau} - \frac{1}{L} \sum_{k=0}^{L/2-1} \cos\left(\frac{2\pi p(2k)}{L}\right) e^{-\frac{4\pi^2(2k)^2}{L^2}\tau}. \end{aligned} \tag{2.54}$$

In the limit $L \to \infty$ and $p \ll L$, the summations above can be approximated as integrals,

$$\begin{aligned}
\frac{1}{L}\sum_{k=0}^{L/2-1} \cos\left(\frac{2\pi pk}{L}\right) e^{-\frac{4\pi^2 k^2}{L^2}\tau} &\approx \frac{1}{2\pi}\int_0^\infty dx \cos(px) e^{-x^2\tau} = \frac{1}{4\sqrt{\pi\tau}} e^{-p^2/4\tau} \\
\frac{1}{L}\sum_{k=0}^{L/2-1} \cos\left(\frac{2\pi p(2k)}{L}\right) e^{-\frac{4\pi^2 (2k)^2}{L^2}\tau} &\approx \frac{1}{4\pi}\int_0^\infty dx \cos(px) e^{-x^2\tau} = \frac{1}{8\sqrt{\pi\tau}} e^{-p^2/4\tau},
\end{aligned} \tag{2.55}$$

which gives the profile of the bond length variables $G_p(t)$ for the dephased, tight-binding lattice setup,

$$\boxed{G_p(t) \approx -\frac{1}{4} + \frac{1}{8\sqrt{\pi\Lambda t}} e^{-p^2/4\Lambda t}} \qquad \text{for} \quad p \ll L. \tag{2.56}$$

Hence the bond length variables exhibit a Gaussian profile. Additionally, recall that $\Lambda = 2J^2/\gamma$ is the effective diffusion constant of the system.

2.3 Bosonic four-point correlator dynamics

The four point correlator on a Bosonic lattice in the site basis is defined as:

$$F_{mnpq}(t) = \mathrm{Tr}\left[\rho(t)\hat{c}_m^\dagger \hat{c}_n^\dagger \hat{c}_p \hat{c}_q\right] \tag{2.57}$$

where $\hat{c}_m(\hat{c}_m^\dagger)$ is the Bosonic annihilation(creation) operator at site m. The microscopic equations for the dynamics of the four-point correlator can be obtained from Eq. (2.3),

$$\begin{aligned}
\frac{d}{dt}F_{mnpq} &= -i\left\langle\left[\hat{c}_m^\dagger \hat{c}_n^\dagger \hat{c}_p \hat{c}_q, \hat{H}\right]\right\rangle + \sum_{i=1}^{L}\gamma\left(\left\langle \hat{n}_i \hat{c}_m^\dagger \hat{c}_n^\dagger \hat{c}_p \hat{c}_q \hat{n}_i\right\rangle - \frac{1}{2}\left\langle\left\{\hat{n}_i^2, \hat{c}_m^\dagger \hat{c}_n^\dagger \hat{c}_p \hat{c}_q\right\}\right\rangle\right) \\
&= i\,J\sum_{j\neq 0}\frac{+F_{mn(p+j)q} + F_{mnp(q+j)} - F_{(m+j)npq} - F_{m(n+j)pq}}{|j|^\mu} \\
&\quad + \gamma\,(\delta_p^m + \delta_q^n + \delta_q^m + \delta_p^n - \delta_n^m - \delta_q^p - 2)F_{mnpq}.
\end{aligned} \tag{2.58}$$

Here, the lattice site indices are understood to be in $\mod L$ arithmetic, a consequence of periodic boundary conditions of lattice setup. The first term on the RHS in the above equation represents the standard unitary contribution and exhibits translational invariance, whilst the second terms contributes to dissipation and represents the local particle number dissipation.

2.3.1 Effective equations for Bosonic four-point correlator dynamics

As described in section 2.2.1, the four-point correlators are the elements of the density matrix confined to the two-particle Hilbert space $\mathcal{H}_2$, when the density matrix is written in the two-particle site basis $\{|mn\rangle\}$, where $|mn\rangle = \hat{c}_m^\dagger \hat{c}_n^\dagger |0\rangle$. The four-point correlator matrix diagonals are identified as the diagonals of the two-particle density matrix in this site basis, and are of the form F_{mnmn} or F_{mnnm}, where $m = n$ is allowed. The standard Bosonic commutation relation confers the following symmetry to the four-point correlators:

$$F_{mnpq} = F_{nmpq} = F_{mnqp} = F_{nmqp} \tag{2.59}$$

Hence, there are $\left(\binom{L}{2} + L\right)^2$ linearly independent four-point correlators, out of which $\binom{L}{2} + L$ are the four-point correlator diagonals. Under the conditions of strong dephasing ($\gamma \gg J$), the off-diagonal elements relax to zero, much before the system attains equilibrium. Hence at late times ($t \gg 1/\gamma$), the dynamics can be effectively described by a classical Markov process involving only the diagonal elements. The off-diagonals can be adibatically eliminated in the slower time scale $\tilde{t} = Jt$, to obtain these equations.

The microscopic dynamical equations of the four-point correlator diagonals of the form $F_{mnmn}(m \neq n)$ reads

$$\frac{d}{dt}F_{mnmn} = +iJ \sum_{j=\pm 1}^{\pm(L/2-1),L} \frac{+F_{mn(m+j)n} + F_{mnm(n+j)} - F_{(m+j)nmn} - F_{m(n+j)mn}}{|j|^\mu}. \tag{2.60}$$

Only the off-diagonals of the four-point correlator matrix appear on the RHS of the above equations. To understand better, the form of these off-diagonals, the summation can be split as follows:

$$\begin{aligned}\frac{d}{dt}F_{mnmn} = &+ iJ \left(\sum_{\substack{j=\pm 1 \\ j\neq n-m}}^{\pm(L/2-1),L} \frac{F_{mn(m+j)n} - F_{(m+j)nmn}}{|j|^\mu} + \frac{F_{mnnn} - F_{nnmn}}{|m-n|^\mu} \right) \\ &+ iJ \left(\sum_{\substack{j=\pm 1 \\ j\neq m-n}}^{\pm(L/2-1),L} \frac{F_{mnm(n+j)} - F_{m(n+j)mn}}{|j|^\mu} + \frac{F_{mnmm} - F_{mmmn}}{|m-n|^\mu} \right)\end{aligned} \tag{2.61}$$

Following the prescription described in section 2.2.1, the off-diagonals appearing the above equation can be obtained in terms of the diagonals:

$$F_{mn(m+j)n} = \frac{iJ}{\gamma}\left[\frac{F_{mnmn} - F_{(m+j)n(m+j)}}{|j|^{\mu}}\right] \qquad F_{mnnn} = \frac{iJ}{\gamma}\left[\frac{F_{mnmn} + F_{mnnm} - F_{nnnn}}{|m-n|^{\mu}}\right]$$

$$F_{(m+j)nmn} = \frac{iJ}{\gamma}\left[\frac{F_{(m+j)n(m+j)n} - F_{mnmn}}{|j|^{\mu}}\right] \qquad F_{nnmn} = \frac{iJ}{\gamma}\left[\frac{F_{nnnn} - F_{mnmn} - F_{nmmn}}{|m-n|^{\mu}}\right]$$

$$F_{mnm(n+j)} = \frac{iJ}{\gamma}\left[\frac{F_{mnmn} - F_{m(n+j)m(n+j)}}{|j|^{\mu}}\right] \qquad F_{mnmm} = \frac{iJ}{\gamma}\left[\frac{F_{mnnm} + F_{mnmn} - F_{mmmm}}{|m-n|^{\mu}}\right]$$

$$F_{m(n+j)mn} = \frac{iJ}{\gamma}\left[\frac{F_{m(n+j)m(n+j)} - F_{mnmn}}{|j|^{\mu}}\right] \qquad F_{mmmn} = \frac{iJ}{\gamma}\left[\frac{F_{mmmm} - F_{nmmn} - F_{mnmn}}{|m-n|^{\mu}}\right] \tag{2.62}$$

Substituting the above in Eq. (2.61) gives the effective equation of motion of four-point diagonals of the form F_{mnmn}, where $(m \neq n)$,

$$\begin{aligned}\frac{d}{dt}F_{mnmn} =& \frac{J^2}{\gamma}\left(2\sum_{j\neq n-m}\frac{F_{(m+j)n(m+j)n} - F_{mnmn}}{|j|^{2\mu}} + \frac{2F_{nnnn} - 2F_{mnmn} - F_{mnnm} - F_{nmmn}}{|m-n|^{2\mu}}\right) \\ & \frac{J^2}{\gamma}\left(2\sum_{j\neq m-n}\frac{F_{m(n+j)m(n+j)} - F_{mnmn}}{|j|^{2\mu}} + \frac{2F_{mmmm} - 2F_{mnmn} - F_{mnnm} - F_{nmmn}}{|m-n|^{2\mu}}\right).\end{aligned} \tag{2.63}$$

Now, the microscopic dynamical equation of the diagonals of the form F_{mmmm} is given as,

$$\frac{d}{dt}F_{mmmm} = +iJ\left(\sum_{j}\frac{F_{mm(m+j)m} + F_{mmm(m+j)} - F_{(m+j)mmm} - F_{m(m+j)mm}}{|j|^{\mu}}\right). \tag{2.64}$$

Following the same prescription as above (and as described in section 2.2.1), the off-diagonals

on the RHS in the above equation can be written in terms of the diagonals,

$$\begin{aligned}
F_{mm(m+j)m} &= \frac{iJ}{\gamma}\left[\frac{F_{mmmm} - F_{(m+j)m(m+j)m} - F_{m(m+j)(m+j)m}}{|j|^{\mu}}\right] \\
F_{mmm(m+j)} &= \frac{iJ}{\gamma}\left[\frac{F_{mmmm} - F_{m(m+j)m(m+j)} - F_{(m+j)mm(m+j)}}{|j|^{\mu}}\right] \\
F_{m(m+j)mm} &= \frac{iJ}{\gamma}\left[\frac{F_{m(m+j)(m+j)m} + F_{m(m+j)m(m+j)} - F_{mmmm}}{|j|^{\mu}}\right] \\
F_{(m+j)mmm} &= \frac{iJ}{\gamma}\left[\frac{F_{(m+j)m(m+j)m} + F_{(m+j)mm(m+j)} - F_{mmmm}}{|j|^{\mu}}\right]
\end{aligned} \tag{2.65}$$

Substituting the above in Eq. (2.64) gives the effective equations of motion of the four-point diagonals F_{mmmm}:

$$\begin{aligned}
\frac{d}{dt}F_{mmmm} = &\frac{2J^2}{\gamma}\sum_{j=\pm 1}^{\pm(L/2-1),L}\left(\frac{F_{m(m+j)m(m+j)} + F_{m(m+j)(m+j)m} - F_{mmmm}}{|j|^{2\mu}}\right) \\
&+ \frac{2J^2}{\gamma}\sum_{j=\pm 1}^{\pm(L/2-1),L}\left(\frac{F_{(m+j)m(m+j)m} + F_{(m+j)mm(m+j)} - F_{mmmm}}{|j|^{2\mu}}\right)
\end{aligned} \tag{2.66}$$

Noting the symmetries of the Bosonic four point correlator, equations (2.63) and (2.66) can be written together as,

$$\boxed{\begin{aligned}
\frac{d}{dt}F_{mnmn} = &\Lambda\left(\sum_{j=\pm 1}^{\pm(L/2-1),L}\frac{(1+\delta_n^m)F_{(m+j)n(m+j)n} - (1+\delta_n^{m+j})F_{mnmn}}{|j|^{2\mu}}\right) \\
&+ \Lambda\left(\sum_{j=\pm 1}^{\pm(L/2-1),L}\frac{(1+\delta_n^m)F_{m(n+j)m(n+j)} - (1+\delta_{n+j}^m)F_{mnmn}}{|j|^{2\mu}}\right),
\end{aligned}} \tag{2.67}$$

where, $\Lambda = 2J^2/\gamma$ can be identified as the diffusion constant. The above equations effectively describe the dynamics of the Bosonic four-point correlator diagonals in time scale $t \gg 1/\gamma$.

2.3.2 Bond length equations for Bosonic four-point correlators

Akin to the case of Fermionic four-point correlator diagonals (Sec. 2.2.2), the "bond length" of a Bosonic four-point correlator diagonal F_{mnmn} is defined as the distance $d(m,n)$ between

lattice sites m and n. On a periodic lattice with L sites, $d(m,n) = \min(|m-n|, L-|m-n|)$, and can take values $\{0, 1, \cdots, L/2\}$. For the alternating state $|\psi_{\text{alt}}\rangle = \prod_{m=1}^{L/2} (\hat{c}_{2m}^{\dagger})^M |0\rangle$, with M bosons on all sites with even indices, all bonds with $d(m,n)$ being odd have one site unoccupied and the other occupied with M bosons. Whilst, all bonds with $d(m,n)$ being even have either both sites unoccupied or both sites occupied with M bosons. These points, along with the translational invariance of the effective equations (Eq. 2.67), support the following claims:

- Given a value $p \in \{1, 3, .., L/2-1\}$, the values of all diagonals $F_{mnmn}(t)$ with bond length $d(m,n) = p$ are identical throughout the dynamics, and we label these as $G_p^{(0)}(t)$. That is, $F_{1212} = F_{2323} = \cdots = F_{L1L1} = G_{(1)}^0$, $F_{1414} = F_{2525} = \cdots = F_{(L-3)1(L-3)1} = G_3^{(0)}$ and so on for $p = 5, 7, \cdots, L/2-1$

- Given a value $p \in \{0, 2, 4, \cdots, L/2\}$, the values of all diagonals $F_{mnmn}(t)$ with (i) bond length $d(m,n) = p$ and (ii) both sites occupied in the initial state are identical throughout the dynamics, and we label these as $G_p^{(1)}$. That is, $F_{2222} = F_{4444} = \cdots = F_{LLLL} = G_0^{(1)}$,$F_{2424} = F_{4646} = \cdots = F_{L2L2} = G_2^{(1)}$ and so on for $p = 4, 6, \cdots, L/2$.

- Given a value $d \in \{2, 4, \cdots, L/2\}$, the values of all diagonals $F_{mnmn}(t)$ with bond length $p(m,n) = d$ and both sites unoccupied in the initial state are identical throughout the dynamics, and we label these as $G_p^{(2)}$. That is, $F_{1111} = F_{3333} = \cdots = F_{(L-1)(L-1)(L-1)(L-1)} = G_0^{(2)}$,$F_{1312} = F_{3535} = \cdots = F_{(L-1)1(L-1)1} = G_2^{(2)}$ and so on for $p = 4, 6, \cdots, L/2$.

The above rules define a bijection between the set of Bosonic four-point correlator diagonals $\{F_{mnmn}\}$ and the set of bond length variables $\left\{G_p^{(0),(1),(2)}\right\}$. Using this map on the effective equations of bosons (Eq. 2.67), and substituting the diagonals F_{mnmn} with appropriate bond length variables $G_p^{(0),(1),(2)}$, gives the following equations,
For $p = 0$:

$$\frac{d}{dt}G_p^{(1)} = 2\Lambda \sum_{\substack{p' \to \text{odd} \\ p' \neq p}} U_{pp'} \left(2G_{p'}^0 - G_p^{(1)}\right) + 2\Lambda \sum_{\substack{p' \to \text{odd} \\ p' \neq p}} U_{pp'} \left(2G_{p'}^{(1)} - G_p^{(1)}\right) \tag{2.68}$$

$$\frac{d}{dt}G_p^{(2)} = 2\Lambda \sum_{\substack{p' \to \text{odd} \\ p' \neq p}} U_{pp'} \left(2G_{p'}^0 - G_p^{(2)}\right) + 2\Lambda \sum_{\substack{p' \to \text{odd} \\ p' \neq p}} U_{pp'} \left(2G_{p'}^{(2)} - G_p^{(2)}\right) \tag{2.69}$$

For $p > 0$:

$$\frac{d}{dt}G_p^0 = 2\Lambda \sum_{\substack{p'\to\text{odd}\\ p'\neq p}} U_{pp'}\left(G_{p'}^0 - (1+\delta_0^{p'})G_p^0\right) + 2\Lambda \sum_{\substack{p'\to\text{odd}\\ p'\neq p}} U_{pp'}\left(\frac{G_{p'}^1 + G_{p'}^2}{2} - (1+\delta_0^{p'})G_p^0\right) \tag{2.70}$$

$$\frac{d}{dt}G_p^{(1)} = 2\Lambda \sum_{\substack{p'\to\text{odd}\\ p'\neq p}} U_{pp'}\left(G_{p'}^0 - (1+\delta_0^{p'})G_p^{(1)}\right) + 2\Lambda \sum_{\substack{p'\to\text{odd}\\ p'\neq p}} U_{pp'}\left(G_{p'}^{(1)} - (1+\delta_0^{p'})G_p^{(1)}\right) \tag{2.71}$$

$$\frac{d}{dt}G_p^{(2)} = 2\Lambda \sum_{\substack{p'\to\text{odd}\\ p'\neq p}} U_{pp'}\left(G_{p'}^0 - (1+\delta_0^{p'})G_p^{(2)}\right) + 2\Lambda \sum_{\substack{p'\to\text{odd}\\ p'\neq p}} U_{pp'}\left(G_{p'}^{(2)} - (1+\delta_0^{p'})G_p^{(2)}\right), \tag{2.72}$$

where $\Lambda = 2J^2/\gamma$ is the diffusion constant, and the elements of the coupling matrix $U_{pp'}$ is given as:

$$U_{pp'} = \begin{cases} \frac{1}{|p'-p|^{2\mu}} & \text{for } p' = 0, L/2 \\ \frac{1}{|p'-p|^{2\mu}} + \begin{cases} \frac{1}{(p+p')^{2\mu}} & \text{for } p+p' \leq L/2 \\ \frac{1}{(L-(p+p'))^{2\mu}} & \text{for } p+p' > L/2 \end{cases} & \text{for } 0 < p' < L/2 \end{cases} \tag{2.73}$$

Particle number fluctuations on a domain $\{1, 2, \cdots, M\}$ of the lattice, $w_M(L,t) = \left\langle \hat{h}^2 \right\rangle - \left\langle \hat{h} \right\rangle^2$ where $\hat{h} = \sum_{i=1}^{M} \hat{n}_i$ counts the number of particles in the domain $\{1, 2, \cdots, M\}$, can be written in terms of the bond length variables as,

$$w_M(L,t) = -MG_0^{(0)} - \sum_{\substack{p=1\\ p\to\text{odd}}}^{M-1} (M-p)G_p^{(0)} - \sum_{\substack{p=1\\ p\to\text{even}}}^{M-1} (M-p)\frac{G_p^{(1)} + G_p^{(2)}}{2} + \sum_{m=1}^{M} D_{mm}\left[1 - \sum_{n=1}^{M} D_{nn}\right], \tag{2.74}$$

where, $D_{mm} = \left\langle \hat{c}_m^\dagger \hat{c}_m \right\rangle$ are the diagonals of the two-point correlator matrix, as defined in Sec. 2.1. In the expression of particle number fluctuation, for bonds of even length, the occupied ($G^{(1)}$) and unoccupied ($G^{(2)}$) bonds contribute equally. Hence, for purposes of computing particle number fluctuation, the following representation can be used:

$$G_p = \begin{cases} G_p^{(0)} & \text{for } p \in \text{odd} \\ \frac{G_p^{(1)} + G_p^{(2)}}{2} & \text{for } p \in \text{even} \end{cases} \tag{2.75}$$

Finally, the equations of the bond length variables $\{G_p\}$ can be obtained via averaging Eqs. (2.68) and (2.69) for $p = 0$ and Eqs. (2.71) and (2.72) for $p > 0$, which gives,

$$\boxed{\frac{d}{dt}G_p = 2\Lambda \sum_{\substack{p'=0 \\ p' \neq p}}^{L/2} U_{pp'} \left((1 + \delta_0^p) G_{p'} - (1 + \delta_0^{p'}) G_p \right),} \tag{2.76}$$

where, the coupling matrix $U_{pp'}$ is as defined in Eq. (2.73). As can be seen, the size of the generator of the bond length equations Eq. (2.76) grows as $\sim L^2$. This provides a significant numerical advantage for computation of four-point correlator dynamics, over the effective (Eq. 2.67) and microscopic (Eq. 2.58) equations, size of the generators of which grow as $\sim L^4$ and $\sim L^8$, respectively.

Chapter 3

Results

3.1 Single particle dynamics

Given the quadratic nature of the Hamiltonian and the jump operators in Eq. (2.2), a single fermion and boson behave identically on the lattice system. Mathematically, this is reflected in the identical equations of motion of the fermionic and bosonic single particle density matrix (Eq. 2.4). Hence, what follows in this section holds for fermions as well as bosons.

To study the dynamics of a single particle on the dephased long-range lattice system, the lattice is initialized in a pure state with a single particle localized at site m_0, $|\psi_0\rangle = \hat{c}^\dagger_{m_0}|0\rangle$. Under the strong dephasing assumption, the effective equations for the single particle density matrix is given by Eq. (2.17). As described in section 2.1.1, the effective equations decouple in the Fourier space, defined as, $\tilde{D}_k = \frac{1}{\sqrt{L}}\sum_{m=1}^{L} e^{-\frac{2\pi i}{L}mk} D_{mm}$, where, k can take values $k \in \{0, 1, \cdots, L-1\}$. Further, the initial state $|\psi_0\rangle = \hat{c}^\dagger_{m_0}|0\rangle$ in the Fourier basis reads as,

$$\tilde{D}_k(t=0) = \frac{1}{\sqrt{L}} e^{-\frac{2\pi i}{L}m_0 k} \tag{3.1}$$

Therefore, the density profile on the lattice, at arbitrary time t, is given by:

$$D_{mm}(t) = \frac{1}{L}\sum_{k=0}^{L-1} e^{\frac{2\pi i}{L}(m-m_0)k} e^{-E(k)t}, \tag{3.2}$$

where, $E(k)$ is the spectrum of the effective equations of the two-point correlator (derived in section 2.1.1) and is given as,

$$E(k) = \Lambda \left(4 \sum_{j=1}^{\frac{L}{2}-1} \frac{\sin^2(\pi jk/L)}{j^{2\mu}} + \frac{1 - e^{i\pi k}}{(L/2)^{2\mu}} \right). \tag{3.3}$$

Here $\Lambda = 2J^2\gamma$ is the diffusion constant of the effective equations of the two-point correlators.

3.1.1 Early time density profile

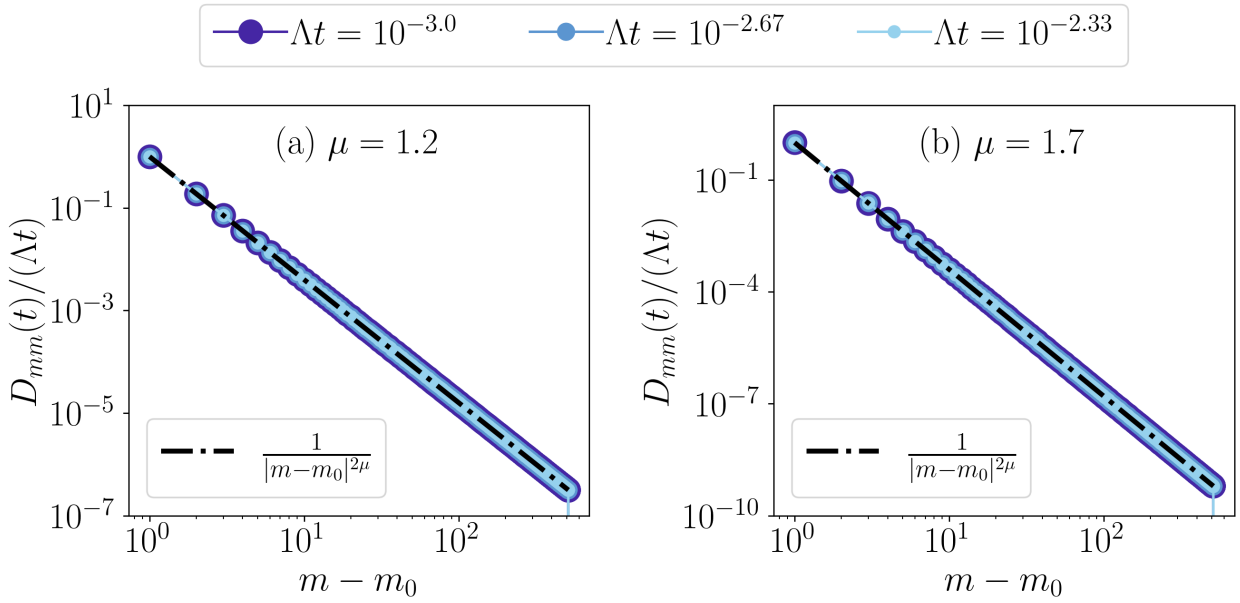

Figure 3.1: Density profile for a single particle initialized at site m_0, at early times ($t \ll 1/\Lambda$), for two different values of hopping exponent (a)$\mu = 1.2$ and (b)$\mu = 1.7$. The hydrodynamic tail $D_{mm} \sim 1/|m - m_0|$ is a characteristic of long-range lattices with power-law hopping.

At early times $t \ll 1/\Lambda$, the propagator $e^{-E(k)t}$ can be approximated till linear order, to give the density profile,

$$\begin{aligned} D_{mm}(t) &= \frac{1}{L} \sum_{k=0}^{L-1} e^{\frac{2\pi i}{L}(m-m_0)k} e^{-E(k)t} \\ &\approx \frac{1}{L} \sum_{k=0}^{L-1} e^{\frac{2\pi i}{L}(m-m_0)k} (1 - E(k)t) = \delta^m_{m_0} - \frac{t}{L} \sum_{k=0}^{L-1} e^{\frac{2\pi i}{L}(m-m_0)k} E(k) \end{aligned} \tag{3.4}$$

The summation on the RHS solves as follows,

$$\begin{aligned}\sum_{k=0}^{L-1} e^{\frac{2\pi i}{L}(m-m_0)k} E(k) &= 4\Lambda \left(\sum_{j=1}^{\frac{L}{2}} \frac{1}{j^{2\mu}} \sum_{k=0}^{L-1} e^{\frac{2\pi i}{L}(m-m_0)k} \sin^2(\pi jk/L) \right) \\ &= 2\Lambda \sum_{j=1}^{\frac{L}{2}} \frac{1}{j^{2\mu}} \sum_{k=0}^{L-1} e^{\frac{2\pi i}{L}(m-m_0)k} (1 - \cos(2\pi jk/L)) \\ &= 2\Lambda \sum_{j=1}^{\frac{L}{2}} \frac{1}{j^{2\mu}} \left(\delta_{m_0}^{m} - \frac{\delta_{m_0}^{m+j} + \delta_{m_0}^{m-j}}{2} \right)\end{aligned} \tag{3.5}$$

Therefore, at early times ($t \ll 1/\Lambda$), the density profile is given as,

$$D_{mm}(t) = \begin{cases} 1 - 2\Lambda t \sum_{j=1}^{L/2} \frac{1}{j^{2\mu}} & \text{for } m = m_0. \\ \frac{\Lambda t}{|m-m_0|^{2\mu}} & \text{for } m \neq m_0. \end{cases} \tag{3.6}$$

Where, m_0 is the site index of the initial excitation. The $\sim 1/|m - m_0|^{2\mu}$ density profile is the so called "hydrodynamic tail" of the excitation, and is a characteristic feature of long range lattices [58, 72]. In fact, these hydrodynamic tails appear at all times on the lattice system, at sites far away from the initial excitation site (Sec. 3.1.2). Figure 3.1 plots the density profile on the lattice system, obtained via numerical integration of the effective equations (Eq. (2.17)), starting from the localized single particle state, clearly showing the presence of hydrodynamic tails at early times ($t \ll 1/\Lambda$).

3.1.2 Density profile at finite time

The effective equation Eq. (2.17) dictates the rate for hopping of the initial excitation at site m_0 to site m, given as

$$W_{m_0 \to m} = \frac{\Lambda}{|m - m_0|^{2\mu}}. \tag{3.7}$$

This rate sets the time scale $\tau(m)$ for hopping of the initial excitation to lattice site m, $\tau(m) = 1/W_{m_0 \to m}$. At arbitrary time t, for lattice sites m far away from the initial excitation, such that $t \ll \tau(m)$, the density profile is governed by single hopping events and is given by the hydrodynamic tails. That is, $D_{mm}(t) = \Lambda t/|m - m_0|^{2\mu}$ for $t \ll \tau(m)$. For lattice sites m near the initial excitation, such that $t \gg \tau(m)$, Refs. [58, 72] provide a solution to the

density profile, which is given as follows,

$$D_{mm}(t) \approx \begin{cases} \frac{1}{8\sqrt{\pi D_\mu t}} e^{-\frac{|m-m_0|^2}{4D_\mu}t} & \text{for } \mu \geq 1.5 \\ \frac{1}{8\pi(D_\mu t)^{-1/(2\mu-1)}} \mathcal{F}_\mu \left(\frac{|m-m_0|}{(D_\mu t)^{1/(2\mu-1)}} \right) & \text{for } \mu \leq 1.5. \end{cases} \tag{3.8}$$

Here, the constant D_μ is proportional to the diffusion constant Λ, and the scaling function $\mathcal{F}_\mu(y)$ is given by, $\mathcal{F}_\mu(y) = \int_{-\infty}^{+\infty} dk\, e^{iyk} e^{-|k|^{1/(2\mu-1)}}$. Therefore, at sites near the excitation, the density profile shows the universal behaviour,

$$D_{mm} = \frac{1}{t^{1/z}} f\left(\frac{|m-m_0|}{t^{1/z}} \right), \tag{3.9}$$

with some scaling function $f(y)$, and the value of the scaling exponent is given as,

$$z = \begin{cases} 2\mu - 1 & \text{for } \mu < 1.5 \\ 2.0 & \text{for } \mu \geq 1.5 \end{cases} \tag{3.10}$$

Figure 3.2 plots the density profile on the lattice system, starting from a single excitation at site m_0 and illustrates (i) the self-similar behavior (Eq. 3.9) of the profile near the initial excitation site m_0 and (ii) hydrodynamic tails $\sim 1/|m-m_0|^{2\mu}$ of the profile at sites far away from m_0.

3.1.3 Moments of the density profile

The n-th moment, $\langle x^n \rangle (t)$, of the density profile $D_{mm}(t)$ of a single exciton initialized at site m_0 is defined as:

$$\langle x^n \rangle (t) = \sum_{m=1}^{L} (m-m_0)^n D_{mm}(t) \tag{3.11}$$

Given the symmetric nature of the density profile $D_{mm}(t)$ about the initial excitation site m_0, all odd moments of the profile are zero at all times. The moments of the distribution may be obtained from the characteristic function $K(q,t)$ of the density profile, defined as, $K(q,t) = \sum_{m=1}^{L} e^{iq(m-m_0)} D_{mm}(t)$, for real number q. Expanding the exponential in the above equation gives the relation between the characteristic function $K(q,t)$ and the moments $\{\langle x^n \rangle (t)\}$ of the profile, $K(q,t) = \sum_{n=0}^{\infty} \frac{(iq)^n}{n!} \langle x^n \rangle (t)$. Therefore the moments can be written

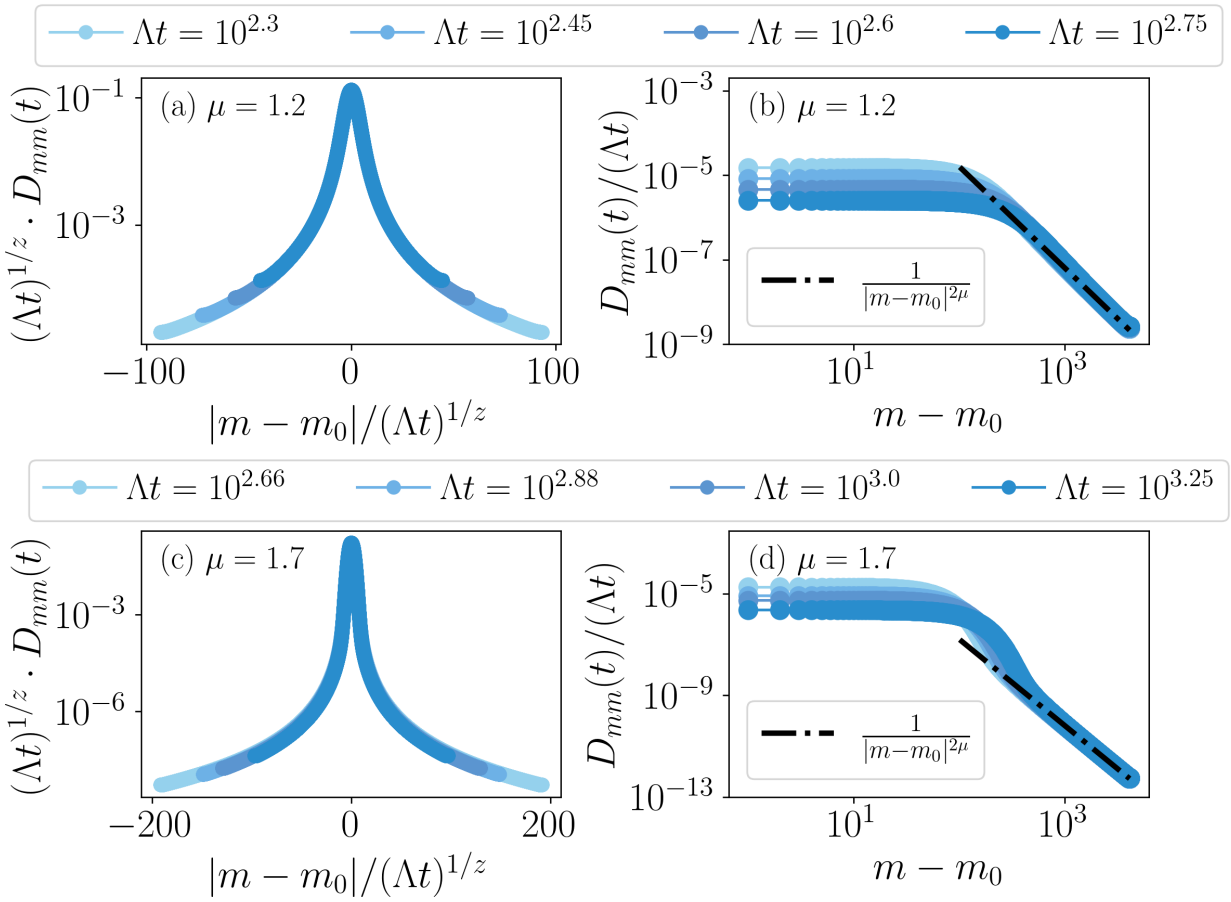

Figure 3.2: Plot for density profile D_{mm} vs $|m - m_0|$ on the lattice system, starting from an initial excitation at m_0, obtained via numerical integration of the effective equations (Eq. (2.17)). (a) and (c) show the scaling behaviour of the density profile, $D_{mm} = \frac{1}{t^{1/z}} f(|m - m_0|/t^{1/z})$, at sites m near the initial excitation site m_0. Scaling the y and x axes by $t^{1/z}$ and $1/t^{1/z}$ shows a perfect collapse amongst the profile $D_{mm}(t)$ at different times, verifying the scaling behaviour. The value of scaling exponent is $z = 2\mu - 1$ for $\mu < 1.5$ and $z = 2.0$ for $\mu \geq 1.5$. (b) and (c) show the hydrodynamic tails of the density profile $D_{mm} = \Lambda t/|m - m_0|^{2\mu}$ at sites m far away from the initial excitation site m_0.

as,

$$\langle x^2 \rangle (t) = -\frac{\partial^2 K(q,t)}{\partial q^2}\bigg|_{q=0}, \quad \langle x^4 \rangle (t) = \frac{\partial^4 K(q,t)}{\partial q^4}\bigg|_{q=0}, \quad \langle x^6 \rangle (t) = -\frac{\partial^6 K(q,t)}{\partial q^6}\bigg|_{q=0} \tag{3.12}$$

and so on, for all even-moments. The equation of motion of the characteristic function can be obtained from the effective equations for the two-point correlator $D_{mm}(t)$. Given the translationally invariant nature of the effective equations, the equations for $K(q,t)$ decouple

in q space, and is given as, $K(q,t) = e^{-E(q)t}$, with $E(q) = 4\Lambda \sum_{j=1}^{L/2} \frac{\sin^2(qj/2)}{j^{2\mu}}$. With this, the temporal growth of even-moments $\langle x^2 \rangle, \langle x^4 \rangle, \langle x^6 \rangle$ can be obtained as,

$$\langle x^2 \rangle (t) = \left. \frac{\partial^2 E(q)}{\partial q^2} \right|_{q=0} t \tag{3.13}$$

$$\langle x^4 \rangle (t) = 3 \left(\left. \frac{\partial^2 E(q)}{\partial q^2} \right|_{q=0} \right)^2 t^2 + \left. \frac{\partial^4 E(q)}{\partial q^4} \right|_{q=0} t \tag{3.14}$$

$$\langle x^6 \rangle (t) = 18 \left(\left. \frac{\partial^2 E(q)}{\partial q^2} \right|_{q=0} \right)^3 t^3 - 24 \left(\left. \frac{\partial^2 E(q)}{\partial q^2} \right|_{q=0} \right) \left(\left. \frac{\partial^4 E(q)}{\partial q^4} \right|_{q=0} \right) t^2 + \left. \frac{\partial^6 E(q)}{\partial q^6} \right|_{q=0} t \tag{3.15}$$

Further, the derivatives of $E(q)$ can be obtained as,

$$\frac{\partial^{2n} E(q)}{\partial q^{2n}} = (-1)^{n+1} \left(2\Lambda \sum_{j=1}^{L/2} \frac{1}{j^{2(\mu-n)}} \right). \tag{3.16}$$

Note that at early times $t \ll 1/\Lambda$, the linear term in Eqs. (3.13)-(3.15) dominates, and as a result, at early times, the moments grow linearly in time. This is illustrated in Fig. 3.3. At late times, the leading order term dominates, which gives the growth $\langle x^{2n} \rangle (t) \sim (Dt)^n$ for even moments, where the constant D can be identified as the effective diffusion constant, and is given as, $D = \left. \frac{\partial^2 E(q)}{\partial q^2} \right|_{q=0}$.

For values of hopping exponent $\mu < 1.5$, the effective diffusion constant D diverges in the thermodynamic limit ($L \to \infty$), a signature of super-diffusive transport in the regime $\mu < 1.5$. Whilst, for values of hopping exponent $\mu \geq 1.5$, the even moments do not diverge in the thermodynamic limit and grow as $\langle x^{2n} \rangle (t) \sim t^n$. This is a signature of diffusive transport in the regime $\mu \geq 1.5$. In fact, in the diffusive regime ($\mu \geq 1.5$), at late times ($\Lambda t \gg 1$), even-moments of the density profile show self similar behaviour in the form of FV scaling (as defined in Eq. 1.3). That is, for $\Lambda t \gg 1$,

$$\langle x^{2n} \rangle = L^{\alpha} f\left(\frac{t}{L^z} \right), \tag{3.17}$$

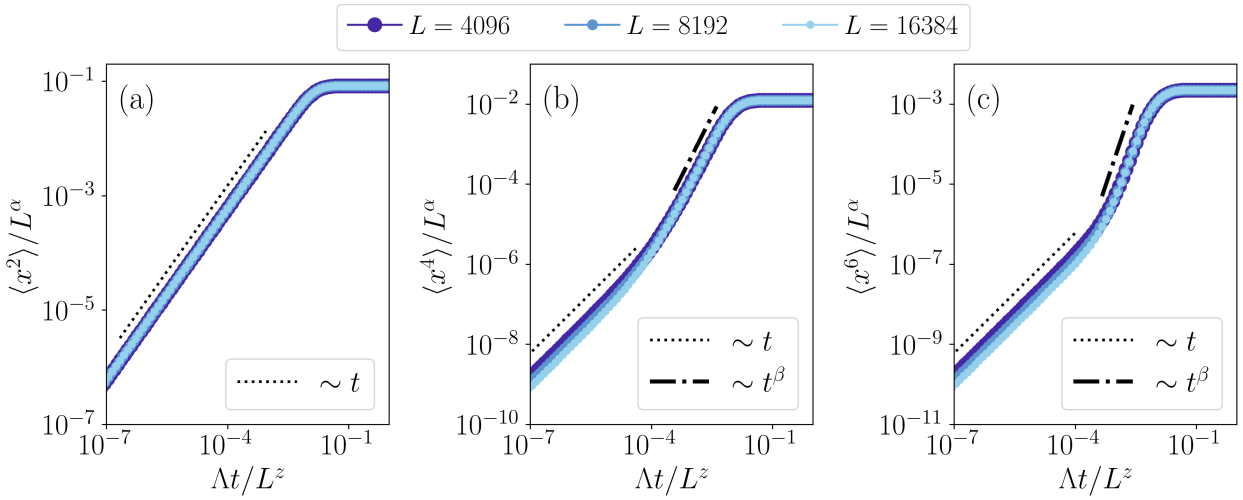

Figure 3.3: Plot for dynamics of even moments $\langle x^{2n} \rangle = \sum_{m=1}^{L} (m - m_0)^{2n} D_{mm}$ of the density profile, obtained numerically. All moments initially grow linearly in time. The collapse in dynamics on scaling the y and x axes with $1/L^\alpha$ and $1/L^z$ respectively, along with t^β growth confirms FV scaling of even moment $\langle x^{2n} \rangle$ with scaling exponents $(\alpha, \beta, z) = (n/2, n/4, 2)$

with some scaling function $f(y)$, that shows the limiting behaviour

$$f(y) = \begin{cases} y^\beta & \text{for } \; y \ll L^z \\ 1 & \text{for } \; y \gg L^z \end{cases}$$

and $z = \alpha/\beta$. The scaling exponents for the even moment $\langle x^{2n} \rangle$ is given by $(\alpha, \beta, z) = (n/2, n/4, 2)$. The limiting behaviour of scaling function $f(y)$, implies the limiting behaviour

$$\langle x^{2n} \rangle \sim \begin{cases} t^\beta & \text{for } \; t \ll t^* \\ L^\alpha & \text{for } \; t \gg t^*, \end{cases} \tag{3.18}$$

where, the saturation time scale t^* shows system size scaling $t^* \sim L^z$. Figure 3.3 plots the dynamics of even moments of the density profile, obtained via numerically via integrating Eq. (2.17), and illustrates (i) the linear growth of the moments for $\Lambda t \ll 1$ (ii) FV scaling of the moments for $\Lambda t \gg 1$.

3.2 Fermionic multi particle dynamics

3.2.1 Particle transport

Particle transport, $P_{\text{tra}}(t)$, is a local observable employed to study multi-particle dynamics for the domain wall initial condition, $|\psi_{\text{D.W.}}\rangle = \prod_{m=1}^{L/2} \hat{c}_m^\dagger |0\rangle$. For such an initial condition particle transport is defined as the number of particles in the right half of the lattice system, i.e., $P_{\text{tra}}(t) = \sum_{m=L/2+1}^{L} D_{mm}(t)$. Under strong dephasing, particle transport dynamics can be obtained via numerical integration of the two-point effective equations.

As illustrated in Fig. 3.4, particle transport dynamics shows universal behaviour in the form of FV scaling, for all values of hopping exponent μ. That is,

$$P_{\text{tra}}(t) = L^\alpha f\left(\frac{t}{L^z}\right) \tag{3.19}$$

with some scaling function $f(y)$, that satisfies the limiting behaviour

$$f(y) = \begin{cases} y^\beta & \text{for } \; y \ll 1 \\ 1 & \text{for } \; y \gg 1 \end{cases}$$

with $\beta = \alpha/z$. This implies the limiting behaviour of $P_{\text{tra}}(t)$,

$$P_{\text{tra}}(t) \sim \begin{cases} t^\beta & \text{for } \; t \ll t^* \\ L^\alpha & \text{for } \; t \gg t^*, \end{cases} \tag{3.20}$$

where, the saturation time scale t^* shows system size scaling $t^* \sim L^z$. Further, the information of the universality class is encoded in the values of the scaling exponents (α, β, z). For $\mu < 1.5$, particle transport dynamics shows super-diffusive scaling with exponents values $(\alpha, \beta, z) = (1.0, 1/(2\mu - 1), 2\mu - 1)$, whilst for $\mu \geq 1.5$, diffusive dynamics is retained with exponent values $(\alpha, \beta, z) = (1.0, 0.5, 2.0)$ (See Fig. 3.4).

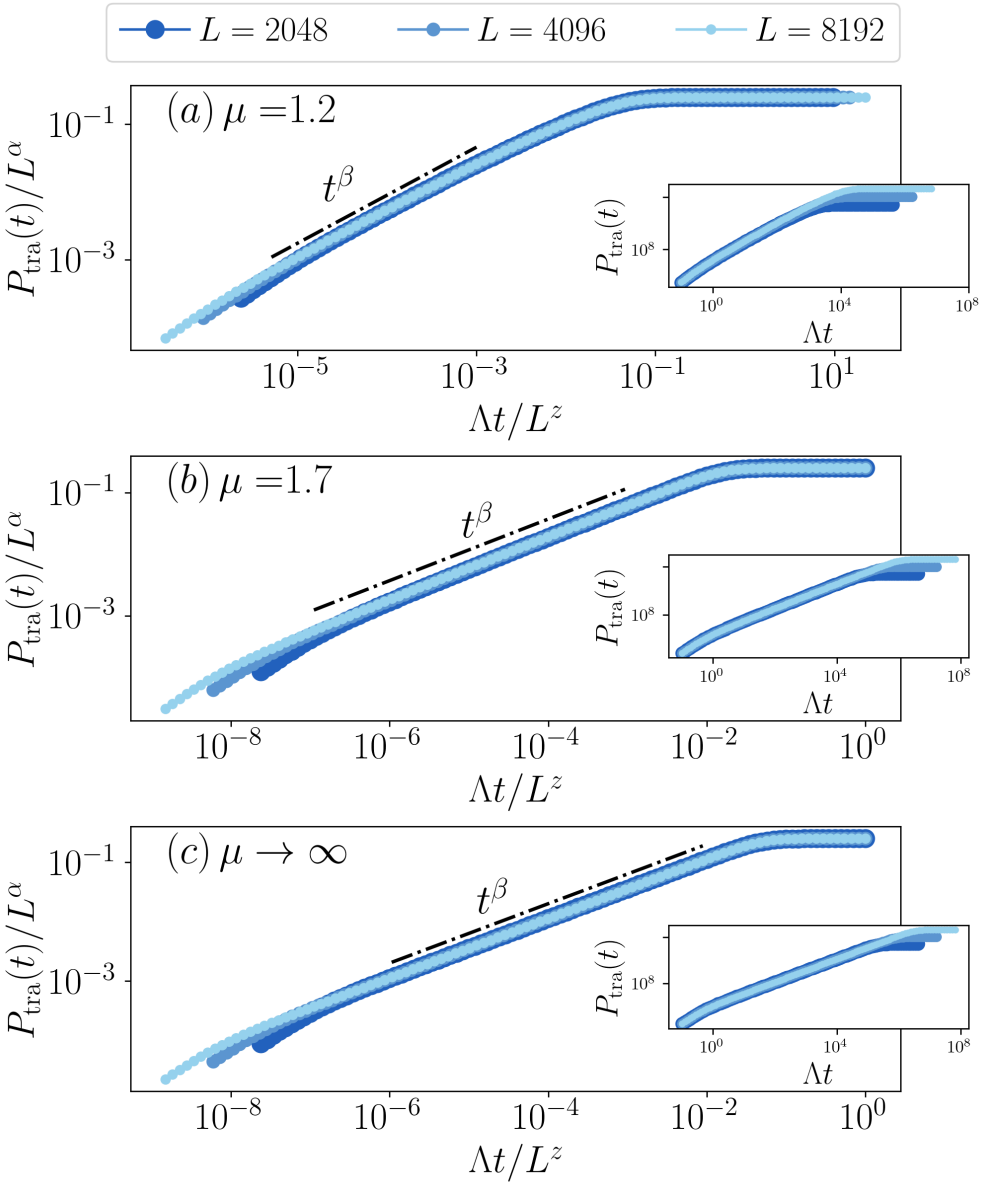

Figure 3.4: Plot for dynamics of particle transport $P_{\rm tra}(t) = \sum_{m=1}^{L/2} D_{mm}(t)$, of fermionic lattices, defined for the domain wall initial state $|\psi_{\rm D.W.}\rangle = \prod_{m=1}^{L/2} \hat{c}_m^\dagger |0\rangle$, for three different values of hopping exponent (a)$\mu = 1.2$,(b)$\mu = 1.7$ and (c)$\mu \to \infty$. The dynamics show a collapse upon scaling the y and x axes by $1/L^\alpha$ and $1/L^z$ respectively, along with an initial $\sim t^\beta$ growth, where $z = \alpha/\beta$. This confirms the FV scaling of the dynamics, with scaling exponents $(\alpha, \beta, z) = (1.0, 1/(2\mu - 1), 2\mu - 1)$ for $\mu < 1.5$ and $(\alpha, \beta, z) = (1.0, 0.5, 2.0)$ for $\mu \geq 1.5$.

3.2.2 Bipartite particle number fluctuation

Bipartite particle number fluctuation, $w(L,t)$, is a multi-particle, non-local observable that quantifies the variance of particle number in one-half of the lattice system. That is, $w(L,t) = \left\langle \hat{h}^2 \right\rangle - \left\langle \hat{h} \right\rangle^2$, where $\hat{h} = \sum_{i=1}^{L/2} \hat{n}_i(t)$ counts the number of particles in one-half of the lattice system. Particle number fluctuation can be written in terms of two-point, $D_{mn} = \left\langle \hat{c}_m^\dagger \hat{c}_n \right\rangle$, and four-point, $F_{mnpq} = \left\langle \hat{c}_m^\dagger \hat{c}_n^\dagger \hat{c}_p \hat{c}_q \right\rangle$, correlators in the site basis. This requires the decomposition of $\left\langle \hat{h}^2 \right\rangle$, in terms of the two and four-point correlator, which can be done as follows,

$$\begin{aligned}
\left\langle \hat{h}^2 \right\rangle &= \sum_{\substack{m,n=1 \\ m\neq n}}^{L/2} \langle \hat{n}_m \hat{n}_n \rangle + \sum_{m=1}^{L/2} \left\langle \hat{n}_m^2 \right\rangle \\
&= \sum_{\substack{m,n=1 \\ m\neq n}}^{L/2} \langle \hat{n}_m \hat{n}_n \rangle + \sum_{m=1}^{L/2} \langle \hat{n}_m \rangle \qquad \text{Since, for fermions } \; \hat{n}_m^2 = \hat{n}_m \\
&= -\sum_{\substack{m,n=1 \\ m\neq n}}^{L/2} \left\langle \hat{c}_m^\dagger \hat{c}_n^\dagger \hat{c}_m \hat{c}_n \right\rangle + \sum_{m=1}^{L/2} \left\langle \hat{c}_m^\dagger \hat{c}_m \right\rangle \\
&= -\sum_{m,n=1}^{L/2} \left\langle \hat{c}_m^\dagger \hat{c}_n^\dagger \hat{c}_m \hat{c}_n \right\rangle + \sum_{m=1}^{L/2} \left\langle \hat{c}_m^\dagger \hat{c}_m \right\rangle \\
&= -\sum_{m,n=1}^{L/2} F_{mnmn} + \sum_{m=1}^{L/2} D_{mm}
\end{aligned} \tag{3.21}$$

Therefore, bipartite particle number fluctuation can be written in terms of two and four-point correlators as,

$$w(L,t) = -\sum_{m,n=1}^{L/2} F_{mnmn}(t) + \sum_{m=1}^{L/2} D_{mm}(t) \left[1 - \sum_{n=1}^{L/2} D_{nn}(t) \right] \tag{3.22}$$

Under the conditions of strong dephasing, the dynamics of F_{mnmn} and D_{mm} can be described by effective equations (2.17) and (2.33), respectively. The effective equation of two-point correlator is given as

$$\frac{d}{dt}D_{mm} = \Lambda \sum_{j=\pm 1}^{\pm(L/2-1),L/2} \frac{D_{(m+j)(m+j)} - D_{mm}}{|j|^{2\mu}} \tag{3.23}$$

which can be solved employing Fourier transform, $\tilde{D}_k = \frac{1}{\sqrt{L}} \sum_{m=1}^{L} e^{-\frac{2\pi i}{L}mk} D_{mm}$ for $k \in \{0, 1, \cdots, L-1\}$, which decouples the effective equations as $\tilde{D}_k(t) = e^{-E(k)t}\tilde{D}_k(0)$, with the spectrum (see Sec. 2.1.1)

$$E(k) = \Lambda \left(4 \sum_{j=1}^{\frac{L}{2}-1} \frac{\sin^2(\pi jk/L)}{j^{2\mu}} + \frac{1 - e^{i\pi k}}{(L/2)^{2\mu}} \right). \tag{3.24}$$

Starting from the alternating initial condition $|\psi_{\text{alt}}\rangle = \prod_{m=1}^{L/2} \hat{c}_{2m}^{\dagger} |0\rangle$, only two Fourier modes, $k = 0, L/2$ are occupied, and the effective equations solve as $D_{mm}(t) = (1 + e^{i\pi m}\, e^{-E(L/2)t})/2$. Further, the particle number in one half of the lattice remains constant, i.e., $\sum_{m=1}^{L/2} D_{mm}(t) = \frac{L}{4}$. Thus, starting from alternating initial state, bipartite particle number fluctuation can be written as

$$w(L,t) = -\sum_{m,n=1}^{L/2} F_{mnmn}(t) + \frac{L}{4}\left[1 - \frac{L}{4}\right] \tag{3.25}$$

The dynamics of four-point correlator diagonals $F_{mnmn}(t)$ is obtained via numerical integration of the bond length equations (Eq. 2.40), which hold for the alternating initial state and are derived in section 2.2.2.

Dynamics of saturation– At times $t \to \infty$, the system density matrix $\hat{\rho}(t)$, undergoing the dynamics as described by the LQME Eq. (**??**), relaxes to the maximally mixed state, i.e., $\lim_{t\to\infty} \hat{\rho}(t) \propto \mathbb{I}$, where $\mathbb{I}$ is the Identity matrix. For the maximally state, the value of the four-point correlator F_{mnmn} is given as, $F_{mnmn} = -(L-2)/(4L-4)$ where $m \neq n$. This gives the saturation value of bipartite number fluctuation,

$$\begin{aligned} \lim_{t\to\infty} w(L,t) &= -\sum_{m,n=1}^{L/2} \lim_{t\to\infty} F_{mnmn}(t) + \frac{L}{4}\left[1 - \frac{L}{4}\right] \\ &= \frac{(L/2)(L/2-1)^2}{2(L-1)} + L/4 - (L/4)^2 \\ &\approx L/4 \qquad\qquad \text{for } \; L \gg 1 \end{aligned} \tag{3.26}$$

The deviation $\Delta(t)$ of the bipartite number fluctuations $w(L,t)$, from its saturation value

$\lim_{t\to\infty} w(L,t)$ is defined as,

$$\Delta(t) = \frac{[\lim_{t\to\infty} w(L,t)] - w(L,t)}{\lim_{t\to\infty} w(L,t)}. \tag{3.27}$$

At late times (i.e., for times when $\Delta(t) < 10^{-2}$), number fluctuation relaxes exponentially to its equilibrium value, with decay rate $\tau_\mu(L)$. This is illustrated in Fig. 3.5(a),(b) and (c), which shows exponential decay of the deviation $\Delta(t)$ when $\Delta(t) < 10^{-2}$, for three different values of hopping exponent μ. The rate of this exponential decay, $\tau_\mu(L)$, shows system size scaling with dynamical exponent z,

$$\tau_\mu(L) \sim L^z \tag{3.28}$$

This system size scaling of the relaxation rate $\tau_\mu(L)$ is illustrated in Fig. 3.5(d). Fig. 3.5(e) plots the values of the dynamical exponent z against the hopping exponent μ. From this, the dependence of the dynamical exponent z on the hopping exponent μ can be concluded to be

$$z = \begin{cases} 2\mu - 1 & \text{for } \mu < 1.5 \\ 2.0 & \text{for } \mu \geq 1.5 \end{cases} \tag{3.29}$$

which indicates super-diffusive non-equilibrium dynamics for $\mu < 1.5$ and diffusive non-equilibrium dynamics for $\mu > 1.5$ with crossover happening at $\mu \sim 1.5$.

Family Viscek (FV) dynamical scaling– Fig. 3.6(a)-(c) plots the dynamics and eventual saturation of bipartite particle number fluctuations $w(L,t)$ for three representative values of the hopping exponent $\mu = 1.2$, $\mu = 1.7$ and $\mu \to \infty$, respectively. For each case, the dynamics for different lattice sizes L exhibit excellent data collapse upon rescaling $w(L,t)$ and t axes by $1/L^\alpha$ and $1/L^z$, respectively, with the saturation exponent $\alpha = 1$ and the dynamical exponent z given by Eq. (3.29). Additionally, at times $t \ll \tau_\mu(L) \sim L^z$, the fluctuations grow as $w(L,t) \sim t^\beta$, with $\beta = \alpha/z$. These results confirm the Family-Vicsek (FV) scaling of bipartite particle number fluctuations, given by

$$w(L,t) = L^\alpha f\left(\frac{t}{L^z}\right), \tag{3.30}$$

where, the scaling function $f(y)$ satisfies the limiting behaviour $f(y) \sim y^\beta$ for $y \ll 1$ and $f(y) \sim 1$ for $y \gg 1$, with $\beta = \alpha/z$. This implies the scaling $\sigma^2(L,t) \sim t^\beta$ in the limit $t \ll L^z$. Thus, particle number fluctuation dynamics show FV scaling with super-diffusive exponents $(\alpha, \beta, z) = (1.0, 1/(2\mu-1), 2\mu-1$ for $\mu < 1.5$ and diffusive scaling exponents

$(\alpha, \beta, z) = (1.0, 0.5, 2.0)$ for $\mu \geq 1.5$. Further, as reported in the appendix C, particle number fluctuation dynamics show FV scaling with the same scaling exponents also for the domain wall initial condition, highlighting the robustness of the universality class with respect to the choice of initial state.

Derivation of Family Viscek (FV) scaling exponents for tight-binding ($\mu \to \infty$) lattice setup

As previously shown, the bipartite particle number fluctuation equilibrates to the saturation value $w(L, t \to \infty) \sim L$. Hence, for all values of hopping exponent, the value of spatial exponent is $\alpha = 1.0$. In section, the bond length representation for the four-point correlator (Sec. 2.2.2) is used to analytically establish the value of the dynamical scaling exponent (z) and diffusive growth of bipartite number fluctuations $w(L, t) \sim t^{\beta}$, with $\beta = 0.5$ for the tight-binding lattice setup.

The bond length equations for the tight-binding lattice (derived in section 2.2.2) can be written as,

$$\frac{d}{dt}|G\rangle = 2\Lambda \mathbf{U}_{\mu\to\infty}|G\rangle, \tag{3.31}$$

Further, in appendix A, it is shown that in the thermodynamic limit ($L \to \infty$) the generator $\mathbf{U}_{\mu\to\infty}$ can be approximated as the symmetric $\tilde{\mathbf{U}}_{\mu\to\infty}$, where,

$$\tilde{\mathbf{U}}_{\mu\to\infty} = \begin{pmatrix} -1 & 1 & 0 & 0 & \dots & 0 & 0 \\ 1 & -2 & 1 & 0 & \dots & 0 & 0 \\ 0 & 1 & -2 & 1 & \dots & 0 & 0 \\ \dots & \dots & \dots & \dots & \dots & \dots & \dots \\ 0 & 0 & \dots & 1 & -2 & 1 & 0 \\ 0 & 0 & 0 & \dots & 1 & -2 & 1 \\ 0 & 0 & 0 & \dots & 0 & 1 & -1 \end{pmatrix}_{L/2\times L/2} . \tag{3.32}$$

The eigenvalues $\left\{\lambda^{(k)}\right\}$ of the symmetrized generator $\tilde{\mathbf{U}}_{\mu\to\infty}$ is given as [96], $\lambda^{(k)} = -4\sin^2\left(\frac{\pi k}{L}\right)$, where $k = 0, 1, \cdots, L/2 - 1$. Further, the alternating initial state, in the eigenbasis of the

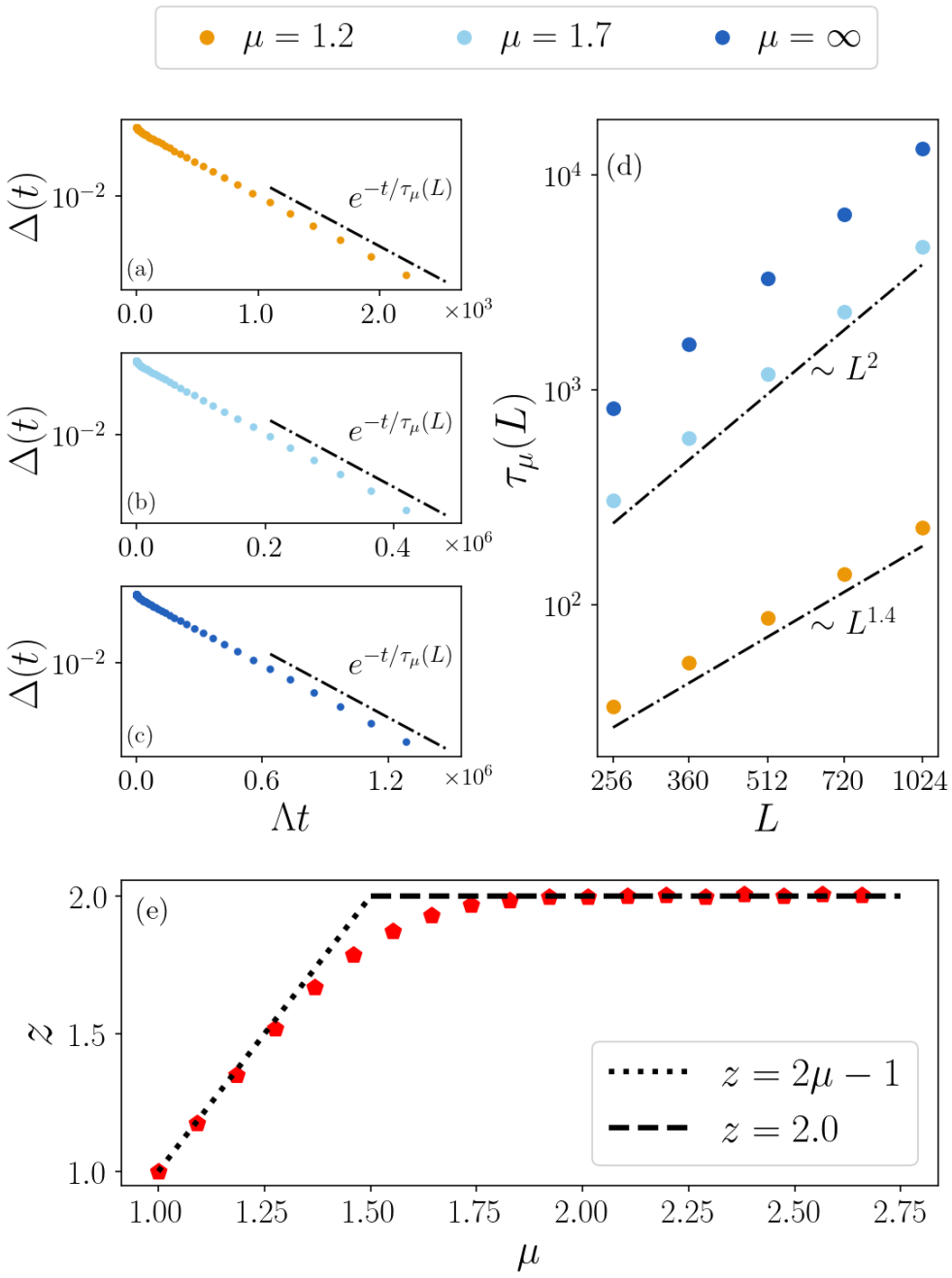

Figure 3.5: (a),(b) and (c): Exponential decay of deviation of particle number fluctuation, defined as $\Delta(t) = 1 - w(L,t)/w(L,t \to \infty)$, for $\Delta(t) \ll 1$, with decay rate $\tau_\mu(L)$. (d) System size scaling of the decay rate $\tau_\mu(L) \sim L^z$, for three different values of hopping exponent $\mu = 1.2$, $\mu = 1.7$ and $\mu \to \infty$. (e) Dependence of dynamical exponent z on hopping exponent μ, showing a crossover from super-diffusive dynamics ($z = 2\mu - 1$) to diffusive dynamics ($z = 2.0$) at $\mu \sim 1.5$

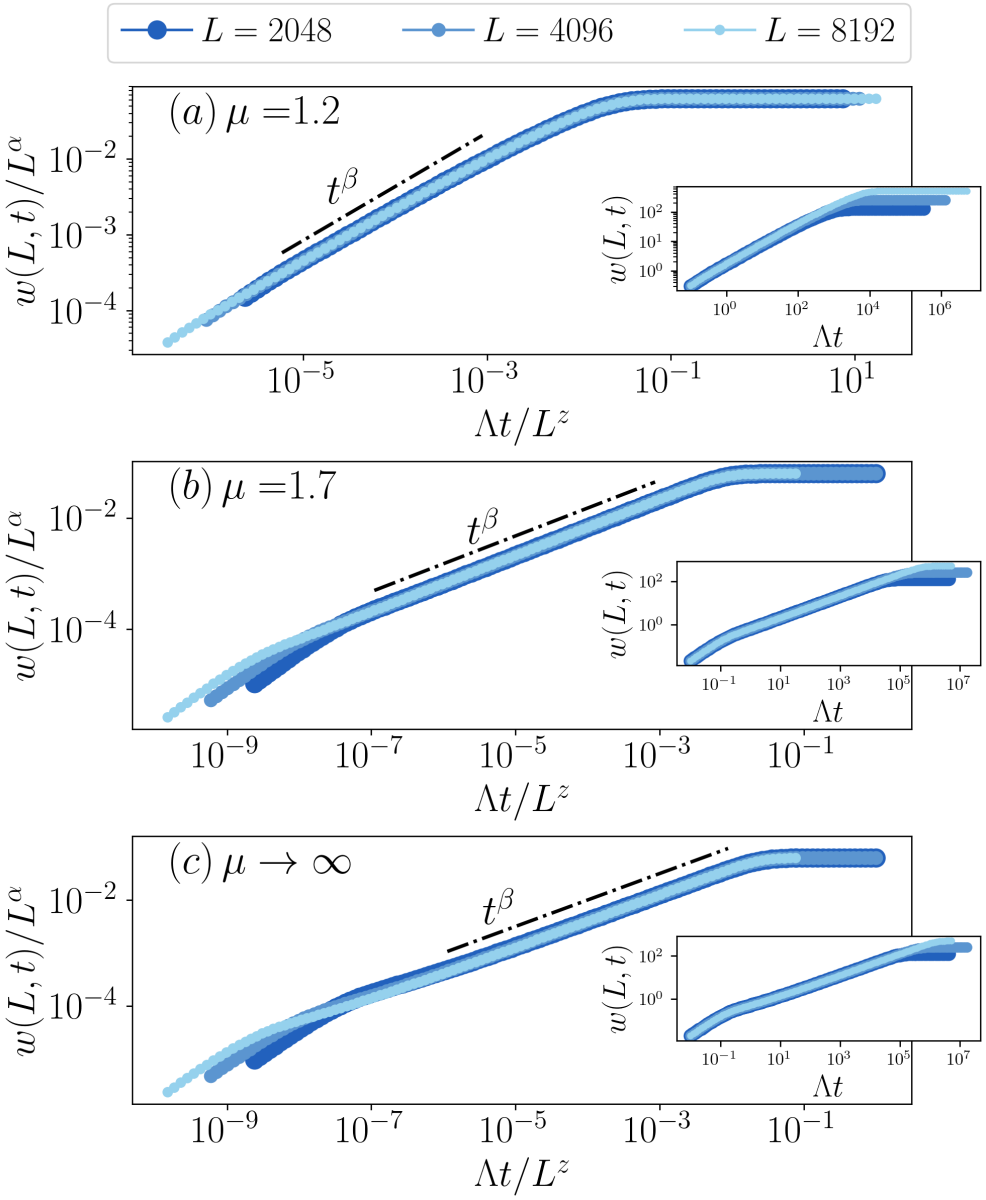

Figure 3.6: Plot for dynamics of bipartite particle number fluctuation $w(L,t) = \left\langle \hat{h}^2 \right\rangle - \left\langle \hat{h} \right\rangle^2$, with $\hat{h} = \sum_{i=1}^{L/2} \hat{n}_i(t)$, of fermionic lattices, starting from the alternating initial state $|\psi_{\text{alt}}\rangle = \prod_{m=1}^{L/2} \hat{c}_{2m}^\dagger |0\rangle$, for three different values of hopping exponent (a)$\mu = 1.2$,(b)$\mu = 1.7$ and (c)$\mu \to \infty$. The dynamics show a collapse upon scaling the y and x axes by $1/L^\alpha$ and $1/L^z$ respectively, along with an initial $\sim t^\beta$ growth, where $z = \alpha/\beta$. This confirms the FV scaling of the dynamics, with scaling exponents $(\alpha, \beta, z) = (1.0, 1/(2\mu - 1), 2\mu - 1)$ for $\mu < 1.5$ and $(\alpha, \beta, z) = (1.0, 0.5, 2.0)$ for $\mu \geq 1.5$.

symmetrized generator $\tilde{\mathbf{U}}_{\mu\to\infty}$, is given as (see Sec. 2.2.2),

$$\tilde{G}_k(\tilde{t}=0) = \begin{cases} -\sqrt{2L}/8 & \text{for } k=0 \\ \begin{cases} 0 & \text{if } k \in \text{even} \\ \frac{\sec(\pi k/L)}{2\sqrt{L}} & \text{if } k \to \text{odd} \end{cases} & \text{for } k>0. \end{cases} \tag{3.33}$$

The time scale of equilibration of the bond length equation (and hence, of bipartite number fluctuation $w(L,t)$) is determined by the lowest occupied non-zero mode. Since the spectrum $\lambda^{(k)}$ satisfies the inequalities $\lambda^{(k)} < 0$ for $k > 0$ and $|\lambda^{(k_1)}| < |\lambda^{(k_2)}|$ for $k_1 < k_2$, the saturation time scale of bipartite number fluctuation, $\tau_{\mu\to\infty}(L)$, is determined by the $k=1$ mode. That is, $\tau_{\mu\to\infty}(L) = 1/\left|\lambda^{(1)}\right|$. In the limit $L \gg 1$, this gives the system size scaling of the saturation time scale, $\tau_{\mu\to\infty}(L) \approx L^2/4\pi^2$. By definition of the dynamical exponent $\tau_{\mu\to\infty}(L) \sim L^z$, one obtains the value of the dynamical exponent $z = 2.0$.

The profile of the bond length variables for the tight binding setup ($\mu \to \infty$) in the thermodynamic limit ($L \to \infty$) at late times ($\Lambda t \gg 1$) is derived in section 2.2.2 to be $G_p(t) = -1/4 + H_p(t)$, where,

$$H_p(t) \approx \frac{1}{8\sqrt{\pi\Lambda t}} e^{-p^2/4\Lambda t} \tag{3.34}$$

Bipartite particle number fluctuation $w(L,t)$ can be written in terms of bond length variables as

$$\begin{aligned} w(L,t) &= -2\sum_{p=1}^{L/2}\left(\frac{L}{2}-p\right)G_p(t) + L/4 - (L/4)^2 \\ &= -2\sum_{p=1}^{L/2}\left(\frac{L}{2}-p\right)\left(-\frac{1}{4}+H_p(t)\right) + L/4 - (L/4)^2 \end{aligned} \tag{3.35}$$

The summation over H_p can be written as follows,

$$\sum_{p=1}^{L/2}\left(\frac{L}{2}-p\right)H_p(t) \approx \frac{L}{2}\sum_{p=0}^{L/2}\frac{e^{-p^2/4\Lambda t}}{8\sqrt{\pi\Lambda t}} - \sum_{p=0}^{L/2} p\frac{e^{-p^2/4\Lambda t}}{8\sqrt{\pi\Lambda t}} - \frac{L}{16\sqrt{\pi t}} \tag{3.36}$$

Since the above expression holds for the limit $\Lambda t \gg 1$, the summations can be approximated

as the following integrals,

$$\sum_{p=1}^{L/2}\left(\frac{L}{2}-p\right)H_p(t) \approx \frac{L}{16\sqrt{\pi}}\int_0^{L/2\sqrt{\Lambda t}} dx e^{-x^2/4} - \frac{\sqrt{\Lambda t}}{8\sqrt{\pi}}\int_0^{L/2\sqrt{\Lambda t}} dx\, x\cdot e^{-x^2/4} - \frac{L}{16\sqrt{\pi\Lambda t}} \tag{3.37}$$

which upon taking the limit $L/\sqrt{\Lambda t} \gg 1$, i.e., $t \ll L^2/\Lambda$ gives,

$$\sum_{p=1}^{L/2}\left(\frac{L}{2}-p\right)H_p(t) \approx \frac{L}{16} - \sqrt{\frac{\Lambda t}{16\pi}} \tag{3.38}$$

Substituting the above in the expression for bipartite number fluctuation (Eq. 3.35) gives,

$$\begin{aligned} w(L,t) &= -2\sum_{p=1}^{L/2}\left(\frac{L}{2}-p\right)G_p(t) + L/4 - (L/4)^2 \\ &= \sum_{p=1}^{L/2}\frac{1}{2} - 2\sum_{p=1}^{L/2}\left(\frac{L}{2}-p\right)H_p(t) + L/4 - (L/4)^2 \\ &\approx L^2/16 - L/8 - L/8 + \sqrt{\Lambda t/(2\pi)} + L/4 - (L/4)^2 \\ &\approx \sqrt{\frac{\Lambda t}{4\pi}} \end{aligned} \tag{3.39}$$

Hence at times $\Lambda t \gg 1$, but much before saturation (i.e., $L/\sqrt{\Lambda t} \gg 1$), bipartite particle number fluctuations grow as $w(L,t) \sim t^{0.5}$, thus confirming the diffusive growth of particle number fluctuations and the value of diffusive exponent $\beta = 0.5$.

3.3 Bosonic multi particle dynamics

3.3.1 Bipartite particle number fluctuations

Akin to the case of fermionic lattices, bipartite particle number fluctuation $w(L,t)$ is defined as the variance of particle number in one half of the lattice system, i.e., $w(L,t) = \left\langle \hat{h}^2 \right\rangle - \left\langle \hat{h} \right\rangle^2$ where $\hat{h} = \sum_{i=1}^{L/2} \hat{n}_i(t)$ counts the number of particles in one half of the lattice. In terms of the bosonic two-point $D_{mn} = \left\langle \hat{c}_m^\dagger \hat{c}_n \right\rangle$ and four-point correlator $F_{mnpq} = \left\langle \hat{c}_m^\dagger \hat{c}_n^\dagger \hat{c}_p \hat{c}_q \right\rangle$, $\left\langle \hat{h}^2 \right\rangle$ can be written as follows,

$$\begin{aligned}
\left\langle \hat{h}^2 \right\rangle &= \sum_{\substack{m,n=1 \\ m\neq n}}^{L/2} \langle \hat{n}_m \hat{n}_n \rangle + \sum_{m=1}^{L/2} \left\langle \hat{n}_m^2 \right\rangle \\
&= \sum_{\substack{m,n=1 \\ m\neq n}}^{L/2} \left\langle \hat{c}_m^\dagger \hat{c}_n^\dagger \hat{c}_m \hat{c}_n \right\rangle + \sum_{m=1}^{L/2} \left\langle \hat{c}_m^\dagger \hat{c}_m \right\rangle \\
&= \sum_{\substack{m,n=1 \\ m\neq n}}^{L/2} \left\langle \hat{c}_m^\dagger \hat{c}_n^\dagger \hat{c}_m \hat{c}_n \right\rangle + \sum_{m=1}^{L/2} \left\langle \hat{c}_m^\dagger \hat{c}_m \hat{c}_m^\dagger \hat{c}_m \right\rangle \\
&= \sum_{\substack{m,n=1 \\ m\neq n}}^{L/2} \left\langle \hat{c}_m^\dagger \hat{c}_n^\dagger \hat{c}_m \hat{c}_n \right\rangle + \sum_{m=1}^{L/2} \left\langle \hat{c}_m^\dagger \hat{c}_m^\dagger \hat{c}_m \hat{c}_m \right\rangle + \sum_{m=1}^{L/2} \left\langle \hat{c}_m^\dagger \hat{c}_m \right\rangle \\
&= \sum_{m,n=1}^{L/2} F_{mnmn} + \sum_{m=1}^{L/2} D_{mm}
\end{aligned} \tag{3.40}$$

Therefore, bipartite particle number fluctuation can be written in terms of two and four-point correlator as,

$$w(L,t) = \sum_{m,n=1}^{L/2} F_{mnmn}(t) + \sum_{m=1}^{L/2} D_{mm}(t) \left[1 - \sum_{n=1}^{L/2} D_{nn}(t) \right] \tag{3.41}$$

The dynamics of bipartite particle number fluctuation is studied under the strong dephasing condition ($\gamma \gg J$), starting from the alternating initial state, defined as $|\psi_{\text{alt}}\rangle = \prod_{m=1}^{L/2} \hat{c}_{2m}^\dagger |0\rangle$. Since the two point correlator for fermions as well as bosons, behave identically, the number of particles in one half the lattice remain constant, i.e., $\sum_{m=1}^{L/2} D_{mm} = L/4$.

And bipartite number fluctuations can be written as, $w(L,t) = \sum_{m,n=1}^{L/2} F_{mnmn}(t) + \frac{L}{4}\left[1 - \frac{L}{4}\right]$. The dynamics of four-point correlator diagonals $F_{mnmn}(t)$ is obtained via numerical integration of the bosonic bond length equations (Eq. 2.76), which are derived in section 2.3.2 and hold for alternating initial state.

Family Viscek (FV) dynamical scaling– Fig. 3.7 plots the dynamics and subsequent saturation of bipartite particle number fluctuations on bosonic lattices, for three representative values of the hopping exponent $\mu = 1.2$, $\mu = 1.7$ and $\mu \to \infty$, respectively. For each value of μ, the excellent collapse in the numerical data for different lattice sizes L upon rescaling the $w(L,t)$ and t axes by $1/L^{\alpha}$ and $1/L^{z}$, along with the initial $w(L,t) \sim t^{\beta}$ growth, confirms the FV scaling of bipartite particle number fluctuations on dephased long-range lattice system consisting of bosons. Further, the value of the scaling exponents (α, β, z) are identical to the case of fermions (see Sec. 3.2.2). That is, $(\alpha, \beta, z) = (1.0, 1/(2\mu - 1), 2\mu - 1)$ for $\mu < 1.5$ and $(\alpha, \beta, z) = (1.0, 0.5, 2.0)$ for $\mu \geq 1.5$. Thus, particle number fluctuation dynamics in bosonic systems exhibit super-diffusive dynamical phase for $\mu < 1.5$ and diffusive dynamical phase for $\mu \geq 1.5$, with the cross-over happening at $\mu \sim 1.5$.

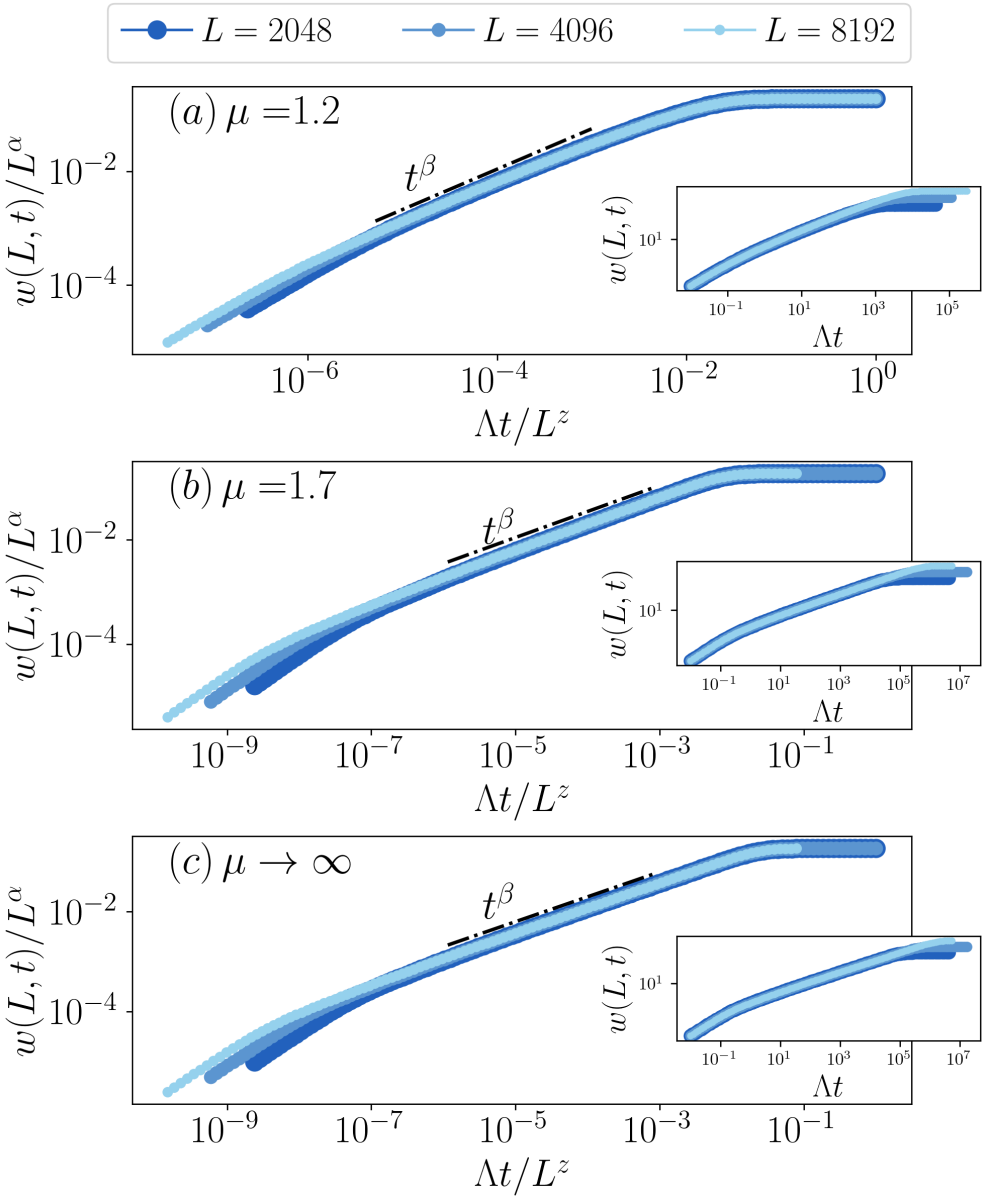

Figure 3.7: Plot for dynamics of bipartite particle number fluctuation $w(L,t) = \left\langle \hat{h}^2 \right\rangle - \left\langle \hat{h} \right\rangle^2$, with $\hat{h} = \sum_{i=1}^{L/2} \hat{n}_i(t)$, of bosonic lattices, starting from the alternating initial state $|\psi_{\text{alt}}\rangle = \prod_{m=1}^{L/2} \hat{c}_{2m}^\dagger |0\rangle$, for three different values of hopping exponent (a)$\mu = 1.2$,(b)$\mu = 1.7$ and (c)$\mu \to \infty$. The dynamics show a collapse upon scaling the y and x axes by $1/L^\alpha$ and $1/L^z$ respectively, along with an initial $\sim t^\beta$ behaviour, where $z = \alpha/\beta$. This confirms the FV scaling of the dynamics, with scaling exponents $(\alpha, \beta, z) = (1.0, 1/(2\mu - 1), 2\mu - 1)$ for $\mu < 1.5$ and $(\alpha, \beta, z) = (1.0, 0.5, 2.0)$ for $\mu \geq 1.5$.

Bibliography

[1] X. Turkeshi and M. Schiró, "Diffusion and thermalization in a boundary-driven dephasing model," *Phys. Rev. B*, vol. 104, p. 144301, Oct 2021.

[2] M. V. Medvedyeva, F. H. L. Essler, and T. c. v. Prosen, "Exact bethe ansatz spectrum of a tight-binding chain with dephasing noise," *Phys. Rev. Lett.*, vol. 117, p. 137202, Sep 2016.

[3] D. A. Abanin, E. Altman, I. Bloch, and M. Serbyn, "Colloquium: Many-body localization, thermalization, and entanglement," *Rev. Mod. Phys.*, vol. 91, p. 021001, May 2019.

[4] J. M. Deutsch, "Quantum statistical mechanics in a closed system," *Phys. Rev. A*, vol. 43, pp. 2046–2049, Feb 1991.

[5] J. M. Deutsch, "Eigenstate thermalization hypothesis," *Reports on Progress in Physics*, vol. 81, p. 082001, jul 2018.

[6] A. Polkovnikov, K. Sengupta, A. Silva, and M. Vengalattore, "Colloquium: Nonequilibrium dynamics of closed interacting quantum systems," *Rev. Mod. Phys.*, vol. 83, pp. 863–883, Aug 2011.

[7] M. Srednicki, "Chaos and quantum thermalization," *Phys. Rev. E*, vol. 50, pp. 888–901, Aug 1994.

[8] M. Ljubotina, M. Žnidarič, and T. c. v. Prosen, "Kardar-parisi-zhang physics in the quantum heisenberg magnet," *Phys. Rev. Lett.*, vol. 122, p. 210602, May 2019.

[9] J. F. Wienand, S. Karch, A. Impertro, C. Schweizer, E. McCulloch, R. Vasseur, S. Gopalakrishnan, M. Aidelsburger, and I. Bloch, "Emergence of fluctuating hydrodynamics in chaotic quantum systems," *Nature Physics*, pp. 1–6, 2024.

[10] M. Hopjan and L. Vidmar, "Scale-invariant survival probability at eigenstate transitions," *Phys. Rev. Lett.*, vol. 131, p. 060404, Aug 2023.

[11] K. Fujimoto and T. Sasamoto, "Exact solution of bipartite fluctuations in one-dimensional fermions," *Phys. Rev. Lett.*, vol. 134, p. 067101, Feb 2025.

[12] E. J. Torres-Herrera, D. Kollmar, and L. F. Santos, "Relaxation and thermalization of isolated many-body quantum systems," *Physica Scripta*, vol. 2015, p. 014018, oct 2015.

[13] R. Nandkishore and D. A. Huse, "Many-body localization and thermalization in quantum statistical mechanics," *Annual Review of Condensed Matter Physics*, vol. 6, no. Volume 6, 2015, pp. 15–38, 2015.

[14] J. Eisert, M. Friesdorf, and C. Gogolin, "Quantum many-body systems out of equilibrium," *Nature Physics*, vol. 11, pp. 124–130, Feb 2015.

[15] L. D'Alessio, Y. Kafri, A. Polkovnikov, and M. R. and, "From quantum chaos and eigenstate thermalization to statistical mechanics and thermodynamics," *Advances in Physics*, vol. 65, no. 3, pp. 239–362, 2016.

[16] A. Sommer, M. Ku, G. Roati, and M. W. Zwierlein, "Universal spin transport in a strongly interacting fermi gas," *Nature*, vol. 472, pp. 201–204, Apr 2011.

[17] S. Erne, R. Bücker, T. Gasenzer, J. Berges, and J. Schmiedmayer, "Universal dynamics in an isolated one-dimensional bose gas far from equilibrium," *Nature*, vol. 563, pp. 225–229, Nov 2018.

[18] P. Ruggiero, P. Calabrese, B. Doyon, and J. Dubail, "Quantum generalized hydrodynamics," *Phys. Rev. Lett.*, vol. 124, p. 140603, Apr 2020.

[19] B. Doyon, J. Dubail, R. Konik, and T. Yoshimura, "Large-scale description of interacting one-dimensional bose gases: Generalized hydrodynamics supersedes conventional hydrodynamics," *Phys. Rev. Lett.*, vol. 119, p. 195301, Nov 2017.

[20] O. A. Castro-Alvaredo, B. Doyon, and T. Yoshimura, "Emergent hydrodynamics in integrable quantum systems out of equilibrium," *Phys. Rev. X*, vol. 6, p. 041065, Dec 2016.

[21] V. B. Bulchandani, R. Vasseur, C. Karrasch, and J. E. Moore, "Bethe-boltzmann hydrodynamics and spin transport in the xxz chain," *Phys. Rev. B*, vol. 97, p. 045407, Jan 2018.

[22] J. Lux, J. Müller, A. Mitra, and A. Rosch, "Hydrodynamic long-time tails after a quantum quench," *Phys. Rev. A*, vol. 89, p. 053608, May 2014.

[23] I. Klich and L. Levitov, "Quantum noise as an entanglement meter," *Phys. Rev. Lett.*, vol. 102, p. 100502, Mar 2009.

[24] D. Gioev and I. Klich, "Entanglement entropy of fermions in any dimension and the widom conjecture," *Phys. Rev. Lett.*, vol. 96, p. 100503, Mar 2006.

[25] H. F. Song, S. Rachel, and K. Le Hur, "General relation between entanglement and fluctuations in one dimension," *Phys. Rev. B*, vol. 82, p. 012405, Jul 2010.

[26] S. Rachel, N. Laflorencie, H. F. Song, and K. Le Hur, "Detecting quantum critical points using bipartite fluctuations," *Phys. Rev. Lett.*, vol. 108, p. 116401, Mar 2012.

[27] U. Agrawal, A. Zabalo, K. Chen, J. H. Wilson, A. C. Potter, J. H. Pixley, S. Gopalakrishnan, and R. Vasseur, "Entanglement and charge-sharpening transitions in u(1) symmetric monitored quantum circuits," *Phys. Rev. X*, vol. 12, p. 041002, Oct 2022.

[28] H. Oshima and Y. Fuji, "Charge fluctuation and charge-resolved entanglement in a monitored quantum circuit with $u(1)$ symmetry," *Phys. Rev. B*, vol. 107, p. 014308, Jan 2023.

[29] A. Lukin, M. Rispoli, R. Schittko, M. E. Tai, A. M. Kaufman, S. Choi, V. Khemani, J. Léonard, and M. Greiner, "Probing entanglement in a many-body–localized system," *Science*, vol. 364, no. 6437, pp. 256–260, 2019.

[30] M. Kiefer-Emmanouilidis, R. Unanyan, J. Sirker, and M. Fleischhauer, "Bounds on the entanglement entropy by the number entropy in non-interacting fermionic systems," *SciPost Phys.*, vol. 8, p. 083, 2020.

[31] "Unlimited growth of particle fluctuations in many-body localized phases," *Annals of Physics*, vol. 435, p. 168481, 2021. Special Issue on Localisation 2020.

[32] D. J. Luitz and Y. B. Lev, "Absence of slow particle transport in the many-body localized phase," *Phys. Rev. B*, vol. 102, p. 100202, Sep 2020.

[33] R. Ghosh and M. Žnidarič, "Resonance-induced growth of number entropy in strongly disordered systems," *Phys. Rev. B*, vol. 105, p. 144203, Apr 2022.

[34] R. Singh, J. H. Bardarson, and F. Pollmann, "Signatures of the many-body localization transition in the dynamics of entanglement and bipartite fluctuations," *New Journal of Physics*, vol. 18, no. 2, p. 023046, 2016.

[35] M. Serbyn, Z. Papić, and D. A. Abanin, "Criterion for many-body localization-delocalization phase transition," *Phys. Rev. X*, vol. 5, p. 041047, Dec 2015.

[36] D. Aceituno Chávez, C. Artiaco, T. Klein Kvorning, L. Herviou, and J. H. Bardarson, "Ultraslow growth of number entropy in an ℓ-bit model of many-body localization," *Phys. Rev. Lett.*, vol. 133, p. 126502, Sep 2024.

[37] K. Fujimoto, R. Hamazaki, and Y. Kawaguchi, "Dynamical scaling of surface roughness and entanglement entropy in disordered fermion models," *Phys. Rev. Lett.*, vol. 127, p. 090601, Aug 2021.

[38] K. Fujimoto, R. Hamazaki, and Y. Kawaguchi, "Family-vicsek scaling of roughness growth in a strongly interacting bose gas," *Phys. Rev. Lett.*, vol. 124, p. 210604, May 2020.

[39] S. Aditya and N. Roy, "Family-vicsek dynamical scaling and kardar-parisi-zhang-like superdiffusive growth of surface roughness in a driven one-dimensional quasiperiodic model," *Phys. Rev. B*, vol. 109, p. 035164, Jan 2024.

[40] D. S. Bhakuni and Y. B. Lev, "Dynamic scaling relation in quantum many-body systems," *Phys. Rev. B*, vol. 110, p. 014203, Jul 2024.

[41] S. Yin, C.-Y. Lo, and P. Chen, "Scaling behavior of quantum critical relaxation dynamics of a system in a heat bath," *Phys. Rev. B*, vol. 93, p. 184301, May 2016.

[42] D. Rossini and E. Vicari, "Scaling behavior of the stationary states arising from dissipation at continuous quantum transitions," *Phys. Rev. B*, vol. 100, p. 174303, Nov 2019.

[43] A. Gleis, S.-S. B. Lee, G. Kotliar, and J. von Delft, "Dynamical scaling and planckian dissipation due to heavy-fermion quantum criticality," *arXiv:2404.14079*, 2024.

[44] H.-C. Kou, Z.-H. Zhang, and P. Li, "Kibble-zurek scaling immune to anti-kibble-zurek behavior in driven open systems at the limit of loss difference," *arXiv: 2411.16406*, 2025.

[45] S. Liu, M.-R. Li, S.-X. Zhang, S.-K. Jian, and H. Yao, "Universal kardar-parisi-zhang scaling in noisy hybrid quantum circuits," *Phys. Rev. B*, vol. 107, p. L201113, May 2023.

[46] D. S. Bhakuni, T. L. M. Lezama, and Y. B. Lev, "Noise-induced transport in the Aubry-André-Harper model," *SciPost Phys. Core*, vol. 7, p. 023, 2024.

[47] K. Fujimoto, R. Hamazaki, and Y. Kawaguchi, "Impact of dissipation on universal fluctuation dynamics in open quantum systems," *Phys. Rev. Lett.*, vol. 129, p. 110403, Sep 2022.

[48] J. M. Kosterlitz, "Phase transitions in long-range ferromagnetic chains," *Phys. Rev. Lett.*, vol. 37, pp. 1577–1580, Dec 1976.

[49] T. Kuwahara and K. Saito, "Area law of noncritical ground states in 1d long-range interacting systems," *Nature Communications*, vol. 11, p. 4478, Sep 2020.

[50] T. Koffel, M. Lewenstein, and L. Tagliacozzo, "Entanglement entropy for the long-range ising chain in a transverse field," *Phys. Rev. Lett.*, vol. 109, p. 267203, Dec 2012.

[51] D. Vodola, L. Lepori, E. Ercolessi, and G. Pupillo, "Long-range ising and kitaev models: phases, correlations and edge modes," *New Journal of Physics*, vol. 18, p. 015001, dec 2015.

[52] C.-F. Chen and A. Lucas, "Finite speed of quantum scrambling with long range interactions," *Phys. Rev. Lett.*, vol. 123, p. 250605, Dec 2019.

[53] M. C. Tran, C.-F. Chen, A. Ehrenberg, A. Y. Guo, A. Deshpande, Y. Hong, Z.-X. Gong, A. V. Gorshkov, and A. Lucas, "Hierarchy of linear light cones with long-range interactions," *Phys. Rev. X*, vol. 10, p. 031009, Jul 2020.

[54] T. Kuwahara and K. Saito, "Strictly linear light cones in long-range interacting systems of arbitrary dimensions," *Phys. Rev. X*, vol. 10, p. 031010, Jul 2020.

[55] T. Zhou, S. Xu, X. Chen, A. Guo, and B. Swingle, "Operator lévy flight: Light cones in chaotic long-range interacting systems," *Phys. Rev. Lett.*, vol. 124, p. 180601, May 2020.

[56] T. Kuwahara and K. Saito, "Absence of fast scrambling in thermodynamically stable long-range interacting systems," *Phys. Rev. Lett.*, vol. 126, p. 030604, Jan 2021.

[57] R. M. Nandkishore and S. L. Sondhi, "Many-body localization with long-range interactions," *Phys. Rev. X*, vol. 7, p. 041021, Oct 2017.

[58] A. G. Catalano, F. Mattiotti, J. Dubail, D. Hagenmüller, T. Prosen, F. Franchini, and G. Pupillo, "Anomalous diffusion in the long-range haken-strobl-reineker model," *Phys. Rev. Lett.*, vol. 131, p. 053401, Aug 2023.

[59] D. S. Bhakuni, L. F. Santos, and Y. B. Lev, "Suppression of heating by long-range interactions in periodically driven spin chains," *Phys. Rev. B*, vol. 104, p. L140301, Oct 2021.

[60] M. Block, Y. Bao, S. Choi, E. Altman, and N. Y. Yao, "Measurement-induced transition in long-range interacting quantum circuits," *Phys. Rev. Lett.*, vol. 128, p. 010604, Jan 2022.

[61] T. Müller, S. Diehl, and M. Buchhold, "Measurement-induced dark state phase transitions in long-ranged fermion systems," *Physical Review Letters*, vol. 128, p. 010605, Jan. 2022. arXiv:2105.08076 [cond-mat, physics:quant-ph].

[62] T. Minato, K. Sugimoto, T. Kuwahara, and K. Saito, "Fate of measurement-induced phase transition in long-range interactions," *Phys. Rev. Lett.*, vol. 128, p. 010603, Jan 2022.

[63] S. Sarkar, B. K. Agarwalla, and D. S. Bhakuni, "Impact of dephasing on nonequilibrium steady-state transport in fermionic chains with long-range hopping," *Phys. Rev. B*, vol. 109, p. 165408, Apr 2024.

[64] A. Dhawan, K. Ganguly, M. Kulkarni, and B. K. Agarwalla, "Anomalous transport in long-ranged open quantum systems," *Phys. Rev. B*, vol. 110, p. L081403, Aug 2024.

[65] E. Zerah Harush and Y. Dubi, "Do photosynthetic complexes use quantum coherence to increase their efficiency? probably not," *Science advances*, vol. 7, no. 8, p. eabc4631, 2021.

[66] G. D. Scholes, "Long-range resonance energy transfer in molecular systems," *Annual review of physical chemistry*, vol. 54, no. 1, pp. 57–87, 2003.

[67] A. Mattioni, F. Caycedo-Soler, S. F. Huelga, and M. B. Plenio, "Design principles for long-range energy transfer at room temperature," *Phys. Rev. X*, vol. 11, p. 041003, Oct 2021.

[68] K. Feron, W. J. Belcher, C. J. Fell, and P. C. Dastoor, "Organic solar cells: understanding the role of förster resonance energy transfer," *International journal of molecular sciences*, vol. 13, no. 12, pp. 17019–17047, 2012.

[69] S. M. Menke and R. J. Holmes, "Exciton diffusion in organic photovoltaic cells," *Energy & Environmental Science*, vol. 7, no. 2, pp. 499–512, 2014.

[70] M. K. Joshi, F. Kranzl, A. Schuckert, I. Lovas, C. Maier, R. Blatt, M. Knap, and C. F. Roos, "Observing emergent hydrodynamics in a long-range quantum magnet," *Science*, vol. 376, no. 6594, pp. 720–724, 2022.

[71] A. Browaeys and T. Lahaye, "Many-body physics with individually controlled rydberg atoms," *Nature Physics*, vol. 16, no. 2, pp. 132–142, 2020.

[72] A. Schuckert, I. Lovas, and M. Knap, "Nonlocal emergent hydrodynamics in a long-range quantum spin system," *Phys. Rev. B*, vol. 101, p. 020416, Jan 2020.

[73] J. Ferreira, T. Jin, J. Mannhart, T. Giamarchi, and M. Filippone, "Transport and nonreciprocity in monitored quantum devices: An exact study," *Phys. Rev. Lett.*, vol. 132, p. 136301, Mar 2024.

[74] P. E. Dolgirev, J. Marino, D. Sels, and E. Demler, "Non-gaussian correlations imprinted by local dephasing in fermionic wires," *Phys. Rev. B*, vol. 102, p. 100301, Sep 2020.

[75] A. Chenu, M. Beau, J. Cao, and A. del Campo, "Quantum simulation of generic many-body open system dynamics using classical noise," *Phys. Rev. Lett.*, vol. 118, p. 140403, Apr 2017.

[76] B. Ghosh, S. Mohanta, M. Kulkarni, and B. K. Agarwalla, "Impact of dephasing probes on incommensurate lattices," *Journal of Statistical Mechanics: Theory and Experiment*, vol. 2024, p. 063101, jun 2024.

[77] A. M. Lacerda, J. Goold, and G. T. Landi, "Dephasing enhanced transport in boundary-driven quasiperiodic chains," *Phys. Rev. B*, vol. 104, p. 174203, Nov 2021.

[78] G. T. Landi, D. Poletti, and G. Schaller, "Nonequilibrium boundary-driven quantum systems: Models, methods, and properties," *Rev. Mod. Phys.*, vol. 94, p. 045006, Dec 2022.

[79] S. Longhi, "Dephasing-induced mobility edges in quasicrystals," *Phys. Rev. Lett.*, vol. 132, p. 236301, Jun 2024.

[80] Y. Liang, C. Xie, Z. Guo, P. Huang, W. Huang, Y. Liu, J. Qiu, X. Sun, Z. Wang, X. Yang, *et al.*, "Dephasing-assisted diffusive dynamics in superconducting quantum circuits," *arXiv:2411.15571*, 2024.

[81] M. Žnidarič, "Exact solution for a diffusive nonequilibrium steady state of an open quantum chain," *Journal of Statistical Mechanics: Theory and Experiment*, vol. 2010, p. L05002, may 2010.

[82] S. Mukamel, "On the nature of intramolecular dephasing processes in polyatomic molecules," *Chemical Physics*, vol. 31, no. 3, pp. 327–333, 1978.

[83] G. Lindblad, "On the generators of quantum dynamical semigroups," *Communications in Mathematical Physics*, vol. 48, no. 2, pp. 119 – 130, 1976.

[84] F. Family and T. Vicsek, "Scaling of the active zone in the Eden process on percolation networks and the ballistic deposition model," *J. Phys. A: Math. Gen.*, vol. 18, pp. L75–L81, Feb. 1985.

[85] T. Vicsek and F. Family, "Dynamic Scaling for Aggregation of Clusters," *Phys. Rev. Lett.*, vol. 52, pp. 1669–1672, May 1984.

[86] T. Vicsek, M. Cserző, and V. K. Horváth, "Self-affine growth of bacterial colonies," *Physica A: Statistical Mechanics and its Applications*, vol. 167, pp. 315–321, Aug. 1990.

[87] C. Gross and W. S. Bakr, "Quantum gas microscopy for single atom and spin detection," *Nature Physics*, vol. 17, pp. 1316–1323, Dec 2021.

[88] M. Rispoli, A. Lukin, R. Schittko, S. Kim, M. E. Tai, J. Léonard, and M. Greiner, "Quantum critical behaviour at the many-body localization transition," *Nature*, vol. 573, pp. 385–389, Sep 2019.

[89] J. F. Sherson, C. Weitenberg, M. Endres, M. Cheneau, I. Bloch, and S. Kuhr, "Single-atom-resolved fluorescence imaging of an atomic mott insulator," *Nature*, vol. 467, pp. 68–72, Sep 2010.

[90] A. Impertro, S. Karch, J. F. Wienand, S. Huh, C. Schweizer, I. Bloch, and M. Aidelsburger, "Local readout and control of current and kinetic energy operators in optical lattices," *arXiv preprint*, 2023.

[91] H. Bernien, S. Schwartz, A. Keesling, H. Levine, A. Omran, H. Pichler, S. Choi, A. S. Zibrov, M. Endres, M. Greiner, V. Vuletić, and M. D. Lukin, "Probing many-body dynamics on a 51-atom quantum simulator," *Nature*, vol. 551, pp. 579–584, Nov 2017.

[92] W. S. Bakr, J. I. Gillen, A. Peng, S. Fölling, and M. Greiner, "A quantum gas microscope for detecting single atoms in a hubbard-regime optical lattice," *Nature*, vol. 462, pp. 74–77, Nov 2009.

[93] L. Christakis, J. S. Rosenberg, R. Raj, S. Chi, A. Morningstar, D. A. Huse, Z. Z. Yan, and W. S. Bakr, "Probing site-resolved correlations in a spin system of ultracold molecules," *Nature*, vol. 614, pp. 64–69, Feb 2023.

[94] E. R. et al, "Dynamics of magnetization at infinite temperature in a heisenberg spin chain," *Science*, vol. 384, no. 6691, pp. 48–53, 2024.

[95] L. K. Joshi, F. Ares, M. K. Joshi, C. F. Roos, and P. Calabrese, "Measuring full counting statistics in a quantum simulator," 2025.

[96] W.-C. Yueh, "Eigenvalues of several tridiagonal matrices.," *Applied Mathematics E-Notes [electronic only]*, vol. 5, pp. 66–74, 2005.

Appendix A

Approximate generator for tight-binding fermionic bond length equations

In section 2.2.2, the bond length equations for the tight-binding ($\mu \to \infty$) lattice setup, $\frac{d}{dt}|G\rangle = 2\Lambda \mathbf{U}_{\mu\to\infty}|G\rangle$, is approximated with the symmetrized generator $\tilde{\mathbf{U}}_{\mu\to\infty}$,

$$\tilde{\mathbf{U}}_{\mu\to\infty} = \begin{pmatrix} -1 & 1 & 0 & 0 & \dots & 0 & 0 \\ 1 & -2 & 1 & 0 & \dots & 0 & 0 \\ 0 & 1 & -2 & 1 & \dots & 0 & 0 \\ \dots & \dots & \dots & \dots & \dots & \dots & \dots \\ 0 & 0 & \dots & 1 & -2 & 1 & 0 \\ 0 & 0 & 0 & \dots & 1 & -2 & 1 \\ 0 & 0 & 0 & \dots & 0 & 1 & -1 \end{pmatrix}_{L/2\times L/2} . \tag{A.1}$$

This section shows that this approximation holds in the thermodynamic limit ($L \to \infty$). The approximation claims that, given an initial state $|G(t=0)\rangle$, the dynamics generated by $\mathbf{U}_{\mu\to\infty}$ and $\tilde{\mathbf{U}}_{\mu\to\infty}$, for a bond length variable $G_p(t)$, converge in the limit $L \to \infty$, provided that p is finite. That is,

$$\lim_{L\to\infty} \langle p| \, e^{\mathbf{U}_{\mu\to\infty} t} \, |G(t=0)\rangle = \lim_{L\to\infty} \langle p| \, e^{\tilde{\mathbf{U}}_{\mu\to\infty} t} \, |G(t=0)\rangle \, , \tag{A.2}$$

where the vector $|p\rangle$, $|p\rangle_j = \delta_p^j$, extracts the p-th element from the dynamics generated by $\mathbf{U}_{\mu\to\infty}$ or $\tilde{\mathbf{U}}_{\mu\to\infty}$.

To show that Eq. (A.2) holds for finite values of p, one needs to show that p-th rows of $e^{\mathbf{U}_{\mu\to\infty}t}$ and $e^{\tilde{\mathbf{U}}_{\mu\to\infty}t}$ are identical in the limit $L\to\infty$. These propagators can be approximated to arbitrary precision by choosing an arbitrary upper cut-off m in the their series expansion,

$$e^{\mathbf{U}_{\mu\to\infty}t} \approx \sum_{n=0}^{m} \frac{1}{n!}\mathbf{U}_{\mu\to\infty}^n t^n \tag{A.3}$$

$$e^{\tilde{\mathbf{U}}_{\mu\to\infty}t} \approx \sum_{n=0}^{m} \frac{1}{n!}\tilde{\mathbf{U}}_{\mu\to\infty}^n t^n \tag{A.4}$$

Further, note that the tridiagonal structure of the generators $\mathbf{U}_{\mu\to\infty}$ and $\tilde{\mathbf{U}}_{\mu\to\infty}$ implies,

$$\langle p|\,\mathbf{U}_{\mu\to\infty}^n = \langle p|\,\tilde{\mathbf{U}}_{\mu\to\infty}^n \qquad \text{for } \; p < L-n. \tag{A.5}$$

Hence, in the limit $L\to\infty$, one may choose arbitrarily high cut-off m in the series expansions Eqs. (A.3) and (A.4), whilst keeping the p-th rows of the propagators identical. Which proves the result,

$$\lim_{L\to\infty} \langle p|\,e^{\mathbf{U}_{\mu\to\infty}t} = \lim_{L\to\infty} \langle p|\,e^{\tilde{\mathbf{U}}_{\mu\to\infty}t} \quad \text{for finite values of } p \tag{A.6}$$

Appendix B

Particle number fluctuation dynamics in closed long-range hopping lattices

In this section, bipartite particle number fluctuations $w(L,t) = \left\langle \hat{h}^2 \right\rangle - \left\langle \hat{h} \right\rangle^2$ on a long-range hopping fermionic lattice, closed to environmental interactions, is studied. The lattice system is modelled by the Hamiltonian given in Eq. (1.1).Given the quadratic nature of the Hamiltonian, applying Wick's theorem, all observables can be written in terms of two-point correlators $D_{mn} = \left\langle \hat{c}_m^\dagger \hat{c}_n \right\rangle$. Bipartite particle number fluctuations can be written in terms of two-point correlators as follows,

$$\begin{aligned} w(L,t) &= \left\langle \left(\sum_{i=1}^{L/2} \hat{n}_i \right)^2 \right\rangle - \left(\left\langle \sum_{i=1}^{L/2} \hat{n}_i \right\rangle \right)^2 \\ &= \sum_{i,j=1}^{L/2} \langle \hat{n}_i \hat{n}_j \rangle - \sum_{i,j=1}^{L/2} \langle \hat{n}_i \rangle \langle \hat{n}_j \rangle \\ &= \sum_{i=1}^{L/2} \left\langle \hat{n}_i^2 \right\rangle + \sum_{\substack{i,j=1 \\ i \neq j}}^{L/2} \langle \hat{n}_i \hat{n}_j \rangle - \sum_{i,j=1}^{L/2} \langle \hat{n}_i \rangle \langle \hat{n}_j \rangle \\ &= \sum_{i=1}^{L/2} \langle \hat{n}_i \rangle + \sum_{\substack{i,j=1 \\ i \neq j}}^{L/2} \langle \hat{n}_i \hat{n}_j \rangle - \sum_{i,j=1}^{L/2} \langle \hat{n}_i \rangle \langle \hat{n}_j \rangle \end{aligned} \tag{B.1}$$

Applying Wick's theorem to the 4 point correlator $\langle \hat{n}_i \hat{n}_j \rangle$ $(i \neq j)$:

$$\langle \hat{n}_i \hat{n}_j \rangle = \left\langle \hat{c}_i^\dagger \hat{c}_i \hat{c}_j^\dagger \hat{c}_j \right\rangle = \left\langle \hat{c}_i^\dagger \hat{c}_i \right\rangle \left\langle \hat{c}_j^\dagger \hat{c}_j \right\rangle - \left\langle \hat{c}_i^\dagger \hat{c}_j \right\rangle \left\langle \hat{c}_j^\dagger \hat{c}_i \right\rangle \tag{B.2}$$

Hence, the last two summations in the expression for $w(L,t)$ solve to:

$$\begin{aligned}
\sum_{\substack{i,j=1 \\ i\neq j}}^{L/2} \langle \hat{n}_i \hat{n}_j \rangle - \sum_{i,j=1}^{L/2} \langle \hat{n}_i \rangle \langle \hat{n}_j \rangle &= \sum_{\substack{i,j=1 \\ i\neq j}}^{L/2} \left\langle \hat{c}_i^\dagger \hat{c}_i \right\rangle \left\langle \hat{c}_j^\dagger \hat{c}_j \right\rangle - \sum_{\substack{i,j=1 \\ i\neq j}}^{L/2} \left\langle \hat{c}_i^\dagger \hat{c}_j \right\rangle \left\langle \hat{c}_j^\dagger \hat{c}_i \right\rangle - \sum_{i,j=1}^{L/2} \left\langle \hat{c}_i^\dagger \hat{c}_i \right\rangle \left\langle \hat{c}_j^\dagger \hat{c}_j \right\rangle \\
&= - \sum_{\substack{i,j=1 \\ i=j}}^{L/2} \left\langle \hat{c}_i^\dagger \hat{c}_i \right\rangle \left\langle \hat{c}_j^\dagger \hat{c}_j \right\rangle - \sum_{\substack{i,j=1 \\ i\neq j}}^{L/2} \left\langle \hat{c}_i^\dagger \hat{c}_j \right\rangle \left\langle \hat{c}_j^\dagger \hat{c}_i \right\rangle \\
&= - \sum_{i,j=1}^{L/2} \left| \left\langle \hat{c}_i^\dagger \hat{c}_j \right\rangle \right|^2
\end{aligned} \tag{B.3}$$

Putting the above solution in the expression for $w(L,t)$ gives,

$$\begin{aligned}
w(L,t) &= \sum_{i=1}^{L/2} \langle \hat{n}_i \rangle - \sum_{i,j=1}^{L/2} \left| \left\langle \hat{c}_i^\dagger \hat{c}_j \right\rangle \right|^2 \\
&= \sum_{i=1}^{L/2} D_{ii}(t) - \sum_{i,j=1}^{L/2} |D_{ij}(t)|^2
\end{aligned} \tag{B.4}$$

Now, the unitary evolution of the two-point correlator can be written as

$$\begin{aligned}
\frac{d}{dt} D_{mn} &= -i \langle \left[\hat{c}_m^\dagger \hat{c}_n, \hat{H} \right] \rangle \\
&= iJ \sum_{j=\pm 1}^{\pm(L/2-1), L/2} \frac{D_{m(n+j)} - D_{(m+j)n}}{|j|^\mu}
\end{aligned} \tag{B.5}$$

The long-range Hamiltonian (Eq (1.1)) exhibits translational invariance and this symmetry is conferred upon the dynamical equations for the two-point correlator Eq. (B.5). Hence, the latter decouple in the momentum space, defined by the Fourier transform, $\tilde{D}_{k_1 k_2} = \frac{1}{L} \sum_{m,n=0}^{L-1} e^{-\frac{2\pi i}{L}(k_1 m + k_2 n)} D_{mn}$, where $k_1, k_2 = 0, 1, \cdots, L-1$. The equations of motion in the

momentum basis can be obtained as follows,

$$\begin{aligned}
\frac{d}{dt}\tilde{D}_{k_1k_2} &= \frac{1}{L}\sum_{m,n=0}^{L-1} e^{-\frac{2\pi i}{L}(k_1m+k_2n)}\frac{d}{dt}D_{mn} \\
&= iJ \sum_{j=\pm1}^{\pm(L/2-1),L/2} \frac{1}{|j|^\mu}\frac{1}{L}\sum_{m,n=0}^{L-1} e^{-\frac{2\pi i}{L}(k_1m+k_2n)}(D_{m(n+j)} - D_{(m+j)n}) \\
&= iJ \sum_{j=\pm1}^{\pm(L/2-1),L/2} \frac{e^{\frac{2\pi i}{L}k_1j}}{|j|^\mu}\frac{1}{L}\sum_{m,n=0}^{L-1} e^{-\frac{2\pi i}{L}(k_1m+k_2n)}D_{mn} \\
&\quad - iJ \sum_{j=\pm1}^{\pm(L/2-1),L/2} \frac{e^{\frac{2\pi i}{L}k_2j}}{|j|^\mu}\frac{1}{L}\sum_{m,n=0}^{L-1} e^{-\frac{2\pi i}{L}(k_1m+k_2n)}D_{mn} \\
&= i(E(k_1) - E(k_2))\tilde{D}_{k_1k_2},
\end{aligned} \tag{B.6}$$

Where $E(k)$ is the spectrum of the Hamiltonian (Eq 1.1), and is given as

$$E(k) = 2J\left(\sum_{j=1}^{L/2-1}\frac{\cos(2\pi kj/L)}{j^\mu} + \frac{e^{i\pi k}}{(L/2)^\mu}\right) \tag{B.7}$$

Hence at arbitrary time t, the two-point correlator in the momentum basis is given as,

$$\tilde{D}_{k_1k_2}(t) = e^{i(E(k_1)-E(k_2))t}\tilde{D}_{k_1k_2}(0) \tag{B.8}$$

The dynamics of bipartite particle number fluctuation $w(L,t)$ is obtained via numerically solving Eq. (B.8). Figure B.1 illustrates the Family-Viscek (FV) dynamical scaling of bipartite particle number fluctuation dynamics, for all values of hopping exponent μ. As opposed to the case of dissipative systems, the value of the hopping exponents has no impact on the universality class of the scaling and the scaling exponents always take ballistic values, $(\alpha, \beta, z) = (1.0, 1.0, 1.0)$.

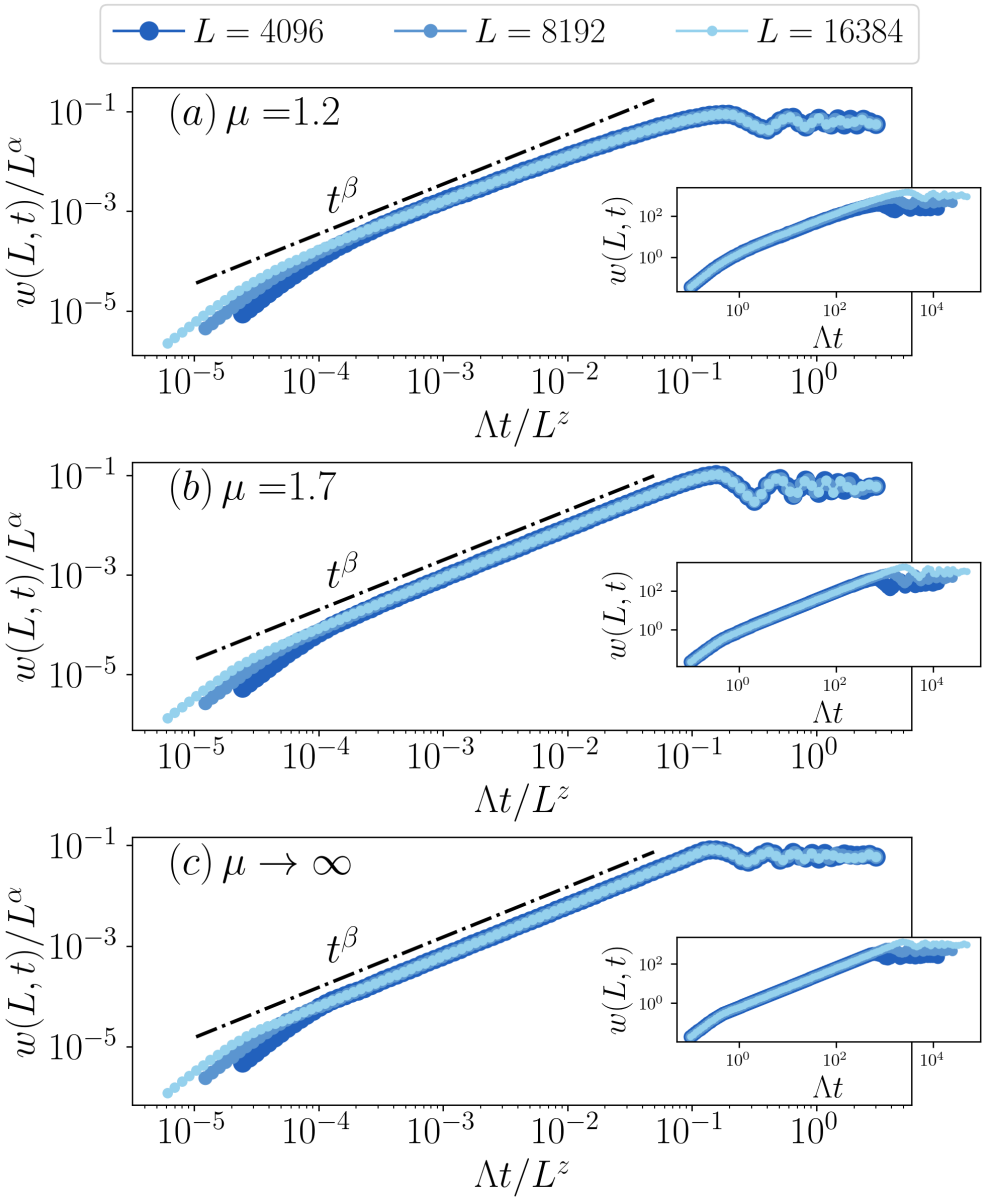

Figure B.1: Plot for dynamics of bipartite particle number fluctuation $w(L,t) = \left\langle \hat{h}^2 \right\rangle - \left\langle \hat{h} \right\rangle^2$, with $\hat{h} = \sum_{i=1}^{L/2} \hat{n}_i(t)$, of free fermionic lattices, starting from the alternating initial state $|\psi_{\text{alt}}\rangle = \prod_{m=1}^{L/2} \hat{c}_{2m}^\dagger |0\rangle$, for three different values of hopping exponent (a)$\mu = 1.2$,(b)$\mu = 1.7$ and (c)$\mu \to \infty$. The dynamics show a collapse upon scaling the y and x axes by $1/L^\alpha$ and $1/L^z$ respectively, along with an initial $\sim t^\beta$ behaviour, where $z = \alpha/\beta$. This confirms the FV scaling of the dynamics, with ballistic scaling exponents $(\alpha, \beta, z) = (1.0, 1.0, 1.0)$ for all values of hopping exponent μ.

Appendix C

Initial state dependence of particle number fluctuation dynamics

In this section, dependence of initial state on the dynamics of bipartite particle number fluctuation on a long-range fermionic lattice (Eq (2.1)) with particle number dephasing at each site (Eq (2.2)) is discussed. In the main text (Sec.3.2.2), Family-Viscek(FV) dynamic scaling of bipartite number fluctuation dynamics, starting from the alternating initial state $|\psi_{\text{alt}}\rangle = \prod_{m=1}^{L/2} \hat{c}_{2m}^{\dagger} |0\rangle$ is established. An initial state that can be taken as extreme example to the alternating state, is the domain wall state, defined as $|\psi_{\text{D.W.}}\rangle = \prod_{m=1}^{L/2} \hat{c}_{m}^{\dagger} |0\rangle$.

Under strong dephasing conditions, the dynamics of the two and four-point correlators can be effectively described by Eqs. (2.17) and (2.33), respectively. These are numerically integrated to obtain the dynamics of bipartite number fluctuation.

Figure C.1(a)-(c) plots the dynamics of bipartite particle number fluctuation, starting from the domain wall initial state, for three representative values of the hopping exponent $\mu = 1.2$,$\mu = 1.7$ and $\mu \to \infty$, respectively. Identical to the case of alternating initial state, particle number fluctuation dynamics starting from the domain wall state show spatio-temporal universality in the form of FV scaling, with the exact same scaling exponents. That is, $(\alpha, \beta, z) = (1.0, 1/(2\mu - 1), 2\mu - 1)$ for $\mu < 1.5$ and $(\alpha, \beta, z) = (1.0, 0.5, 2.0)$ for $\mu \geq 1.5$. This result, thus highlights the robustness of the FV scaling universality of particle number fluctuation against the choice of initial conditions.

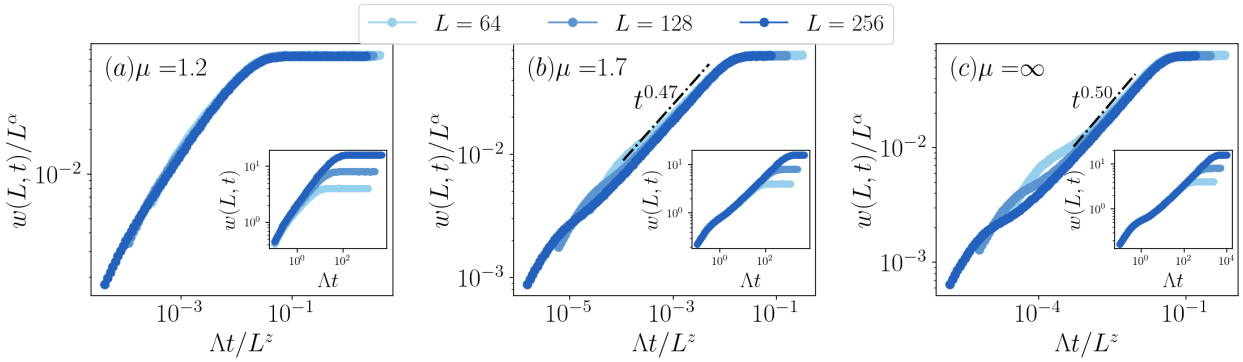

Figure C.1: Family-Viscek(FV) scaling of bipartite particle number fluctuation $w(L,t)$ dynamics, starting from the domain wall initial state. For (a)$\mu < 1.5$ the scaling exponents are super-diffusive, whilst for (b),(c)$\mu \geq 1.5$ the scaling exponents are diffusive. Note that in the super-diffusive regime, (a)$\mu = 1.2$, the initial super-diffusive growth $\sim t^{\beta}$ is not observed due to finite-size effects in small lattice sizes ($L \sim 10^2$).